DESIGN AND IMPLEMENTATION OF AN OUTDOOR HIGH-SPEED OPTICAL WIRELESS LINK

A Thesis Submitted

in Partial Fulfillment of the Requirements

for the Degree of

Master of Technology

by

Major Saju Thomas

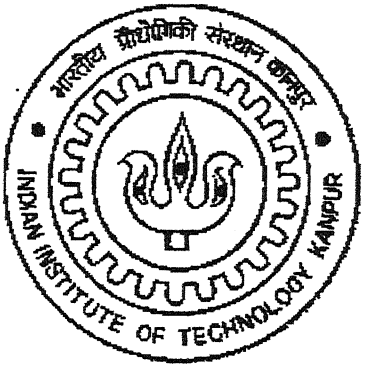

to the

DEPARTMENT OF ELECTRICAL ENGINEERING

INDIAN INSTITUTE OF TECHNOLOGY KANPUR

DECEMBER, 2001

CERTIFICATE

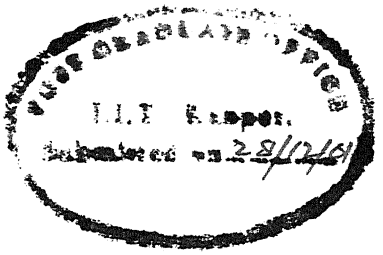

It is certified that the work contained in the thesis entitled **"DESIGN AND IMPLEMENTATION OF AN OUTDOOR HIGH-SPEED OPTICAL WIRELESS LINK"**, by Maj Saju Thomas, has been carried out under my supervision and that this work has not been submitted elsewhere for a degree.

December 2001

(Dr. Joseph John)
Associate Professor
Department of Electrical Engineering
Indian Institute of Technology
Kanpur.

ABSTRACT

Free space optical communication is a cost effective, high-bandwidth, wireless alternative for the last mile connectivity of high-speed data to the user premises. The thesis deals with the design issues and implementation details of a high-speed outdoor optical wireless link. A detailed review of related work in this field has been done. Various considerations in the design of an outdoor optical wireless links are discussed. An experimental outdoor high-speed optical wireless link with 20 Mbps data rate and a link length of 20 m has been established using discrete components. The transmitter uses a low cost 'key-chain' laser as the source. The receiver is PIN diode based, with a JFET as the front-end amplifying device. In this thesis, the design and realization of a low noise feedback receiver with particular attention to the preamplifier stage is dealt with in detail. Circuit simulation of the preamplifier stage using Micro-cap is also included. Simulated results are also compared with actual measured parameters.

ACKNOWLEDGEMENTS

It is really a pity that good hardware engineers with sound theoretical knowledge have become 'endangered species', with the MNCs pumping money into the software fields.

I consider it a boon, to have got a chance to work in the hardware side, especially under the supervision of Dr Joseph John, a genius that belongs to the above category and acquire whatever possible, in this short span of six months. I am really indebted to him for sparing his precious time out of his tight schedule and for his guidance, 'without reproach'

Let me take this opportunity to express my gratitude to my parents, especially my beloved father, the late Shri Thomas Varghese, for inspiring and introducing me into the world of electronics, who had himself assembled a RF receiver half a century back!

I am grateful to my colleague and lecturer, Mrs Nisha Kuruvilla for the valuable discussions and the unselfish helps rendered from time to time in spite of a busy schedule in this campus.

Thanks are also due to Mr.S.K. Kole and the staff of the PCB lab for making the PCBs in time, and of course to Ram Birbal for helping me with the soldering and Sanjay for all the lab assistance rendered.

Last but not the least; let me thank my better half, Laly for bearing the burdens of my studies at IIT Kanpur and in helping me with the manuscript of this thesis.

Saju Thomas

To

My Lord and my God

CONTENTS

CHAPTER 1

INTRODUCTION

In the past few years, the growth of data communications has been enormous. Almost all data communication has been established using wired physical connections, such as optical fibres and coaxial cables. These physical connections introduce difficulties in construction and rewiring during the system set up and expansion phases. Also, users are not happy about being tied to a desk or a fixed location. An alternative that achieves the same goal for data communication while offering mobility is the wireless communication. Traditionally, radio frequency transmission was used in wireless applications. However, the RF spectrum is so congested that it is very difficult to accommodate new high bit rate applications.

1.1 OPTICAL WIRELESS COMMUNICATION

In 1993, the Infra red Data Association (IrDA) was founded, whose role is to promote the commercialization of the optical wireless communication technology, set the standards and bring together the interested parties. They have broadly classified the optical wireless systems into *long distance systems* (>500m), *short distance systems* (1m-500m) and *very short distance systems* (1m or less) [15]. In this thesis, we will be restricting ourselves to short distance systems used as an outdoor link.

Optical wireless communication can provide a line of sight, wireless, high bandwidth communication link between two sites, say for example neighboring buildings. Data is transmitted by modulated light in a fashion similar to fiber optic cable transmission. Instead of a contained glass channel, however, the beam travels through the atmosphere.

Optical wireless communication has many advantages over other wireless technologies, such as microwave or radio frequency (RF). They are:

a) High data rate.

b) Increased security.

c) No FCC licensing or frequency allocation required.

d) Portable and quickly deployable.

e) Economic.

The primary disadvantage of optical wireless communication is its vulnerability to atmospheric effects such as attenuation and scintillation, which can reduce link availability and may introduce burst errors. The narrow transmission beam also makes alignment of the laser communication terminal more difficult than the wider beam RF systems.

1.2 THESIS OBJECTIVE

The objective of this thesis work is to study the various aspects of outdoor wireless links and to design and implement an experimental out door high-speed optical wireless link. This involves the following tasks:

- Review of the subject and a thorough understanding of the various aspects of wireless optical communication.
- Design and implementation of a low noise receiver.
- Design and implementation of a cheap laser transmitter.
- Circuit simulation of the designed circuits.
- PCB design of the transmitter and the receiver.
- Establishing an experimental link outdoors with the prototype made.

1.3 THESIS STRUCTURE

Chapter 2 gives a review of the outdoor optical wireless communication systems reported so far. It includes a comparison table of the various optical wireless systems.

Chapter 3 is devoted to the various design issues of outdoor optical wireless links. A detailed study on PIN diode based receiver design and also the design of a cheap and simple laser transmitter are given.

Chapter 4 gives the various aspects of hardware implementation. Detailed circuit diagrams of the implemented circuits are given. Implementation details, such as PCB design, precautions to be taken in handling laser diodes, etc are discussed. The chapter

also gives SPICE modeling, simulation and analysis using Micro-cap and these are compared with actual measured results.

The thesis is concluded in Chapter 5, in which the results and suggestion for future work are also included.

CHAPTER 2

REVIEW OF OUTDOOR OPTICAL WIRELESS LINKS

Trends in the telecommunications and computer industries suggest that the network of the future will consist of a fiber-optic backbone with short-range wireless communication links providing network access to portable communicators and portable computers. In this vision of the future, users moving from room to room will have access to the same high-speed network services available to the wired terminals. This all-optical network will consist of both indoor as well as outdoor optical links. Non-directed infrared links, which are Class-1 eye safe, are used in the indoor links whereas directed high power infrared links, generally lasers of Class-3B eye safety, are used in the outdoor links.

2.1 A BASIC OUTDOOR OPTICAL WIRELESS LINK

A basic outdoor optical communication link is shown schematically in Fig 2.1[3]. It consists of an optical transmitter emitting P_t watts of power into a solid angle of Ω_t steradians and an optical receiver with a collection aperture area of A_r m^2. The distance R between the transmitter and the receiver can range from a few tens of meters (for inter building links), through several tens of thousands of kilometers (for intersatellite links), to several astronomical units- and possibly even farther- in deep-space applications. In addition to the transmitter and the receiver, outdoor optical communication systems include subsystems to perform functions such as beam manipulation, viz. acquisition and tracking.

In an outdoor optical communication link, assuming ideal conditions, viz. perfect alignment of transmitter and receiver, lossless optical components and detectors, the

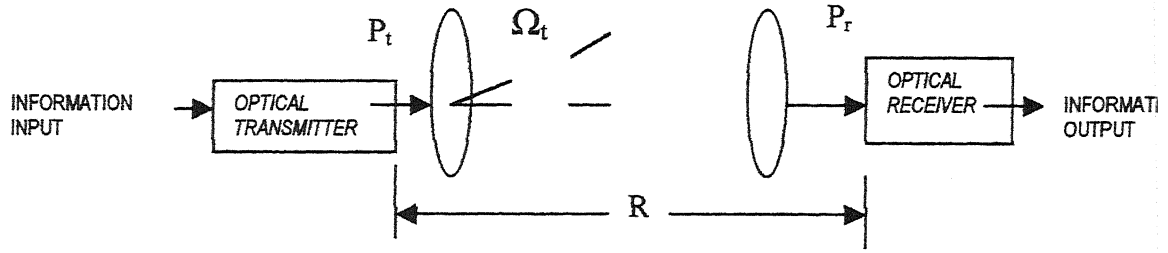

Fig. 2.1. Basic schematic of an outdoor optical wireless link.

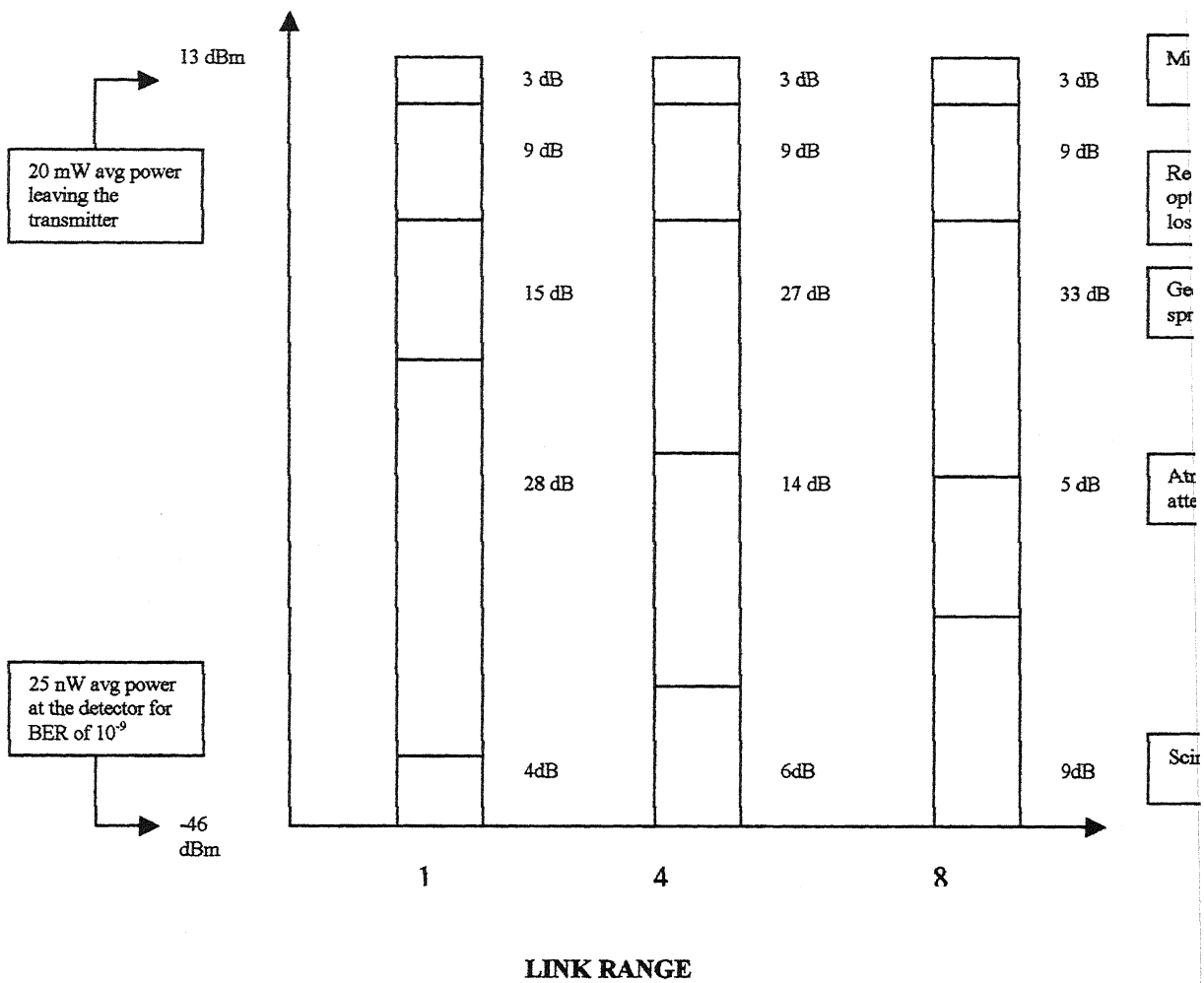

Fig. 2.2. A typical power link budget.

received power, P_r is determined by the formula [3]

$$P_r = P_t \frac{A_r}{\Omega_t R^2} \qquad \text{.....(2.1)}$$

When the real life conditions are taken into account, the right hand side of equation 2.1 has to be multiplied by several inefficiency factors, such as mis-pointing errors, receiver optical losses, geometrical spreading loss, atmospheric attenuation and scintillation (atmospheric turbulence). A typical laser power link budget is shown in Fig 2.2 for a 155 Mb/s transmission rate [13].

Unlike optical fiber communication systems, out door optical links require the transmitter and receiver to be spatially aligned in order to maintain communication. Thus an important step in establishing the link involves the process of beam acquisition. The transmitted beam has to be pointed in the direction of the receiver. A beacon source operating at a different wavelength from that of the transmitter at or near the receiver is often used to designate the correct direction. Alternately, in duplex systems each transmitter can serve as a beacon to the other terminal. The optical receiver has to be pointed in the approximate direction of the transmitter, and then some scanning has to be done until the transmitted beam is within the field of view of the tracking detector. Most receivers employ separate detectors to assist in the beam manipulation functions. These detectors usually have a larger field of view and a lower sensitivity than the optical detector that detects the information signal. Beam acquisition can be simplified by using detector arrays with a large number of elements (e.g. CCD with or without light amplification stages) that can stare into a large field of view. Once the beam is acquired, the alignment is maintained using the spatial information derived from the tracking detector.

2.2 THE TRANSMITTER

The conversion of a low-level electrical signal to a corresponding light intensity envelope in the time domain is accomplished at the transmitter.

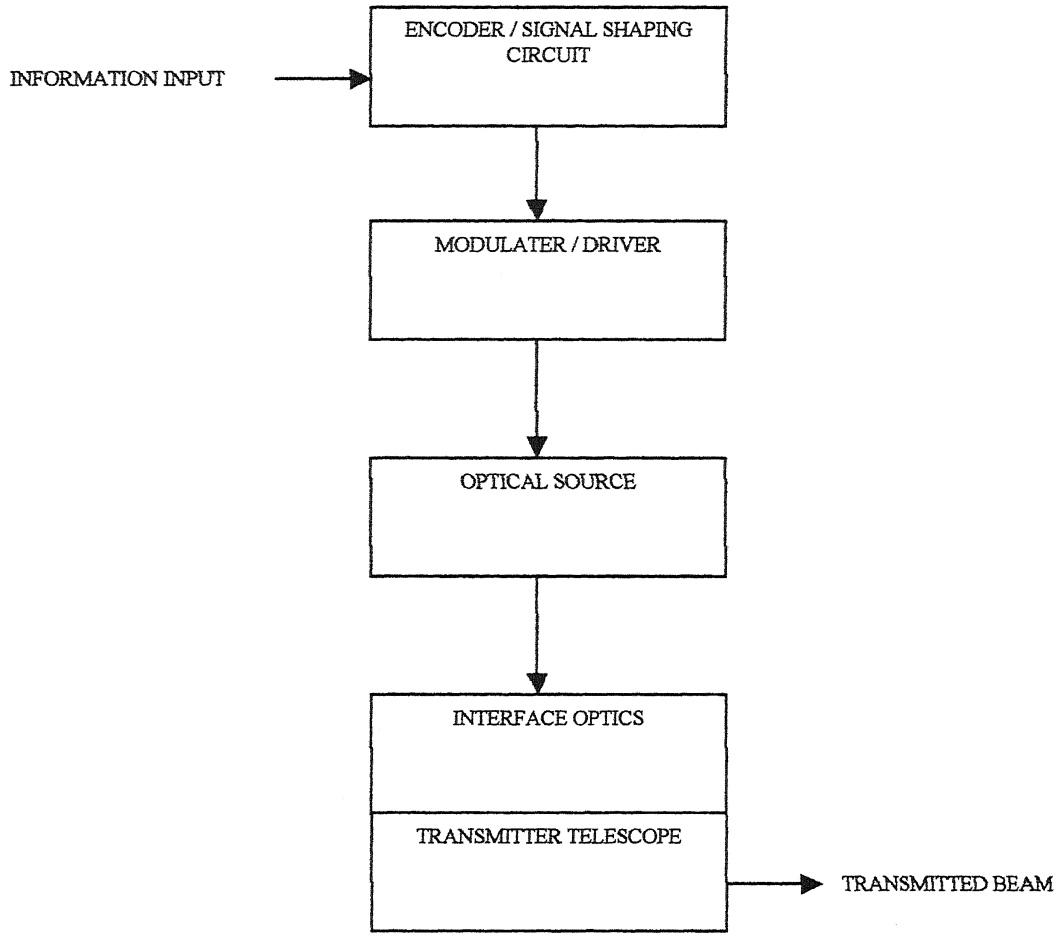

Fig. 2.3. Transmit Terminal.

2.2.1 SYSTEM REQUIREMENT

The transmit terminal equipment will essentially consist of an information encoder or signal shaping circuit preceding a modulation or electronic driver stage which operates the optical source as shown in Fig. 2.3. The interface optics and the transmitter telescope are optional.In order to transmit information optically, it is necessary to modulate a property of the light with the information signal. This property may be intensity, frequency, phase or polarization (direction). Either Intensity Modulation (IM) /

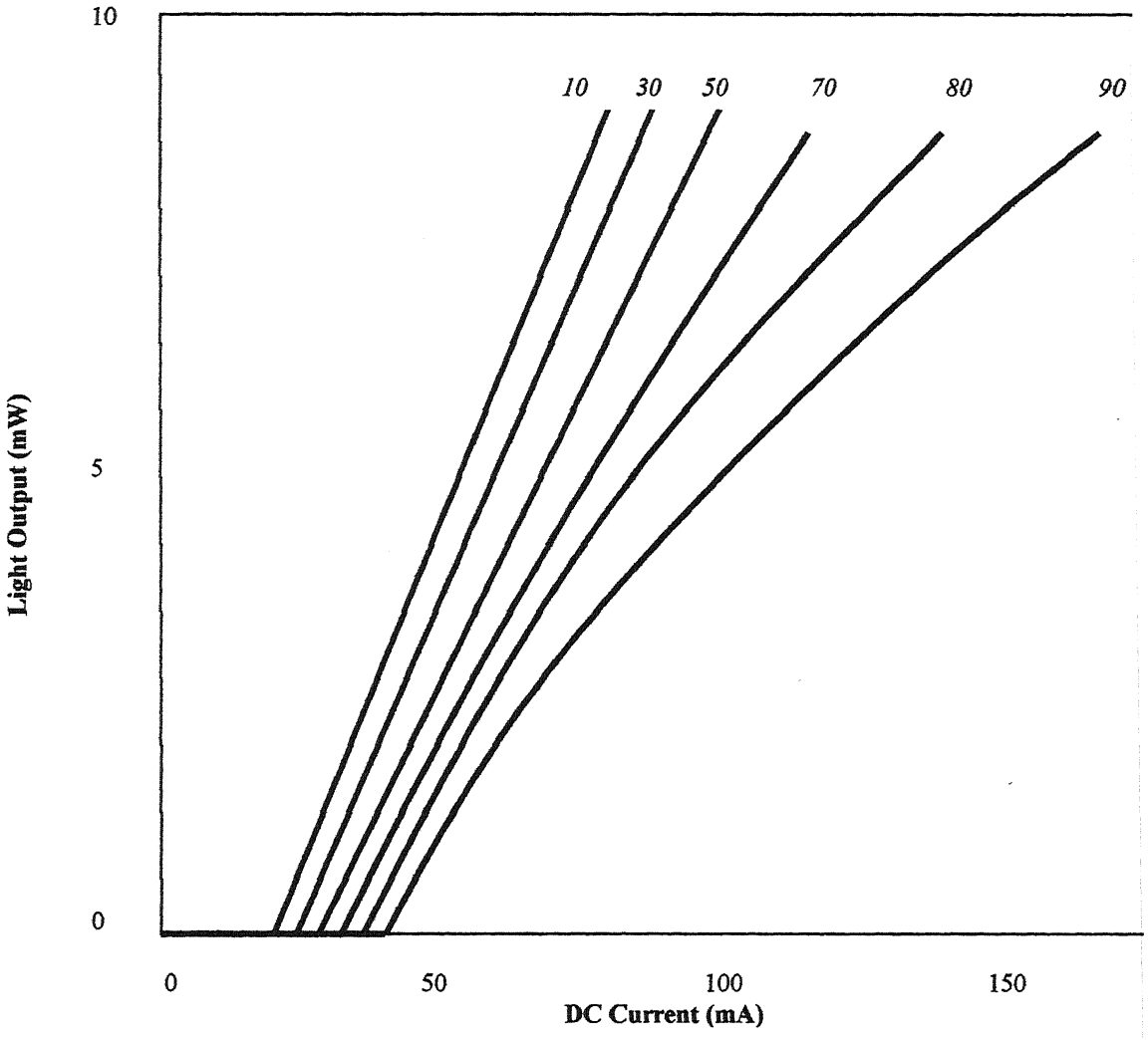

Fig. 2.4. Injection laser output as a function of current and temperature.

Direct Detection (DD) schemes or Coherent optical communication system can be employed for this purpose. However, at present the former scheme is preferred due to its simplicity.

Intensity modulation is easy to implement with the electro luminescent sources available at present (LEDs and injection lasers). The devices can be directly modulated simply by variation of their drive currents at rates up to several gigahertz. However, considering the recent interest in integrated optical devices, it is likely that external

optical modulation may be utilized more in the future in order to achieve greater bandwidth and to allow the use of non-semiconductor sources.

2.2.2 THE PROBLEMS

For intensity modulated light wave transmitters, two semiconductor devices-light emitting diodes (LEDs) and injection laser diodes are suitable in terms of size, speed, efficiency, and electrical characteristics. But because of the broad spectral width (50-150 nm full width at half maximum amplitude) of LEDs, they are generally used only for short distance, lower bit rate applications whereas semiconductor lasers offer narrow spectral width (<10 nm) and hence are suitable for long distance, high bit rate applications. We will be restricting the discussion to semiconductor lasers only.

A typical laser light output versus current (L-I) transfer characteristics for several temperatures is shown in Fig. 2.4. When the diode current is below threshold (I_{th}) cavity and mirror losses exceed the gain derived from stimulated emission and lasing oscillation does not occur. The corresponding light output is the incoherent, spontaneous emission characteristic of an LED. The frequency response of this sub-threshold output is also LED like, being inversely proportional to the spontaneous recombination lifetime of the injected minority carriers.

Beyond threshold, lasing results in efficient conversion of input current to output light, seen as the high differential quantum efficiency (%) or slope efficiency (W/A) of the L-I curve. In this region, the emission is spectrally narrow and has an extended high frequency response.

Since threshold is determined by the gain/loss balance in the laser, I_{th} responds sensitively to temperature or aging induced changes in either gain or loss. Temperature can affect gain or loss through numerous mechanisms (e.g. current spreading and heterobarrier heights). Empirically, threshold current is found to rise with increasing temperature according to $I_{th} \propto \exp \frac{T}{T_0}$, where the characteristic temperature T_0 ranges from 40 to 70 K for InGaAsP lasers.

Long term aging of lasers usually results in irreversible increase in threshold due to a variety of causes. The causes can be separated into three areas: **facet** (mirror)

damage; **ohmic contact degradation;** and **internal failure,** which include dark line defect (DLD) formation. Facet damage and contact degradation become more important as the power level of the device is increased. These mechanisms and others may result in lower slope efficiency as well. Therefore changes in laser characteristics may be allowed for in the design of a transmitter.

Facet Damage: Attempts to operate semiconductor lasers at high powers can result in gross damage to the cleaved facets that act as mirrors. This is believed to be due to a high surface state recombination rate which prevents the facet surface from being inverted, thus causing absorption of laser light. This can either melt the mirror surface in a catastrophic manner or propagate dark lines and other defects into the active region. The critical peak optical power density for catastrophic mirror damage is approximately 10^6 W/cm^2 for CW operation and about 10^7 W/cm^2 for pulsed operation with very short pulses (<100 ns). Interestingly, the longer wavelength InGaAsP semiconductor laser does not seem to have a limit on the optical power density at the facet. This may be due to the lower recombination rate at the surface of InGaAsP.

Ohmic Contact Degradation: The deterioration of ohmic contacts is a problem common to all semiconductor devices and is observed under certain conditions in transistors, rectifiers, and other components subjected to either high current densities or high temperatures. Because the threshold current of laser diodes is fairly temperature dependent, an increase in thermal and/or electrical resistance affects the laser performance. In laser diodes, the thermal resistance of the contact between the laser chip and the heat sink tends to increase with time. This degradation process depends on the solder used, the current density through the contacts, and the temperature. The increase in thermal resistance of the contact produces an increase in the junction temperature for a given operating current. Thus it is possible to observe a decrease in the CW output of a laser operated at a constant current that is directly caused by this effect.

Internal Damage: Internal damage in the laser often appears as dark line defects (DLD). A DLD is a network of dislocations that can form during laser operating in the region of the active cavity. Once started, it can grow extensively in a few hours. The initiation of DLD can take much longer. The DLD produces relatively high absorption and is a region with a high density of nonradiative recombination centers. The growth of

DLD is accompanied by an increase in the threshold current and a decrease in the external differential quantum efficiency.

Modal Partition Noise: When operated continuously (CW) above threshold, multilongitudinal mode lasers show a spectrum characterized by several wavelengths (modes) spaced according to the dimension of the Fabry-Perot cavity. When the diode forward current is modulated at high frequencies, many multilongitudinal mode lasers develop additional modes. In addition to resulting in a wider spectrum, the modes have a probability of exchanging power with each other. Whether or not additional modes appear, modulation induces 'noisy' statistical power fluctuations (modal partition noise or MPN) among the modes already present. Because these fluctuations in amplitude and wavelength are chromatically time-dispersed during transmission, jitter and eye closure are observed at the receiver, leading to a sensitivity penalty.

Chirp: Fast changes in laser current also induce unwanted spectral effects by modulating the refractive index of the cavity. The resulting 'chirp' of the emitted wavelength is chromatically dispersed, leading again to power penalties at high bit rates.

Delay: For digital applications, it is important to maximize the energy in the 1 or mark level and minimize the energy in the 0 or space level. The ratio of these two intensities is the extinction ratio or contrast ratio γ. High values of γ cannot be obtained arbitrarily, since the 1 level is usually subject to peak power limitations of the laser set by reliability considerations, and the 0 level is determined by the laser turn on dynamics or spontaneous emission near threshold. Suppose a laser initially has a zero bias (current or voltage) applied to it. If the current is now rapidly increased to a level corresponding to the desired power for the 1 state, a delay between the leading edge of the current pulse and the light output is observed. The delay is accompanied by a transient overshoot (ringing) in the light output, again arising from the dynamics of the coupled carrier and photon populations in the cavity. This delay t_d is given by [3]

$$t_d = \tau_{th} \ln \frac{I}{I - I_{th}} \qquad (2.2)$$

where I is the magnitude of the current pulse and τ_{th} is the carrier recombination lifetime at threshold (usually 2-5ns). The delay can be reduced by making the drive current large

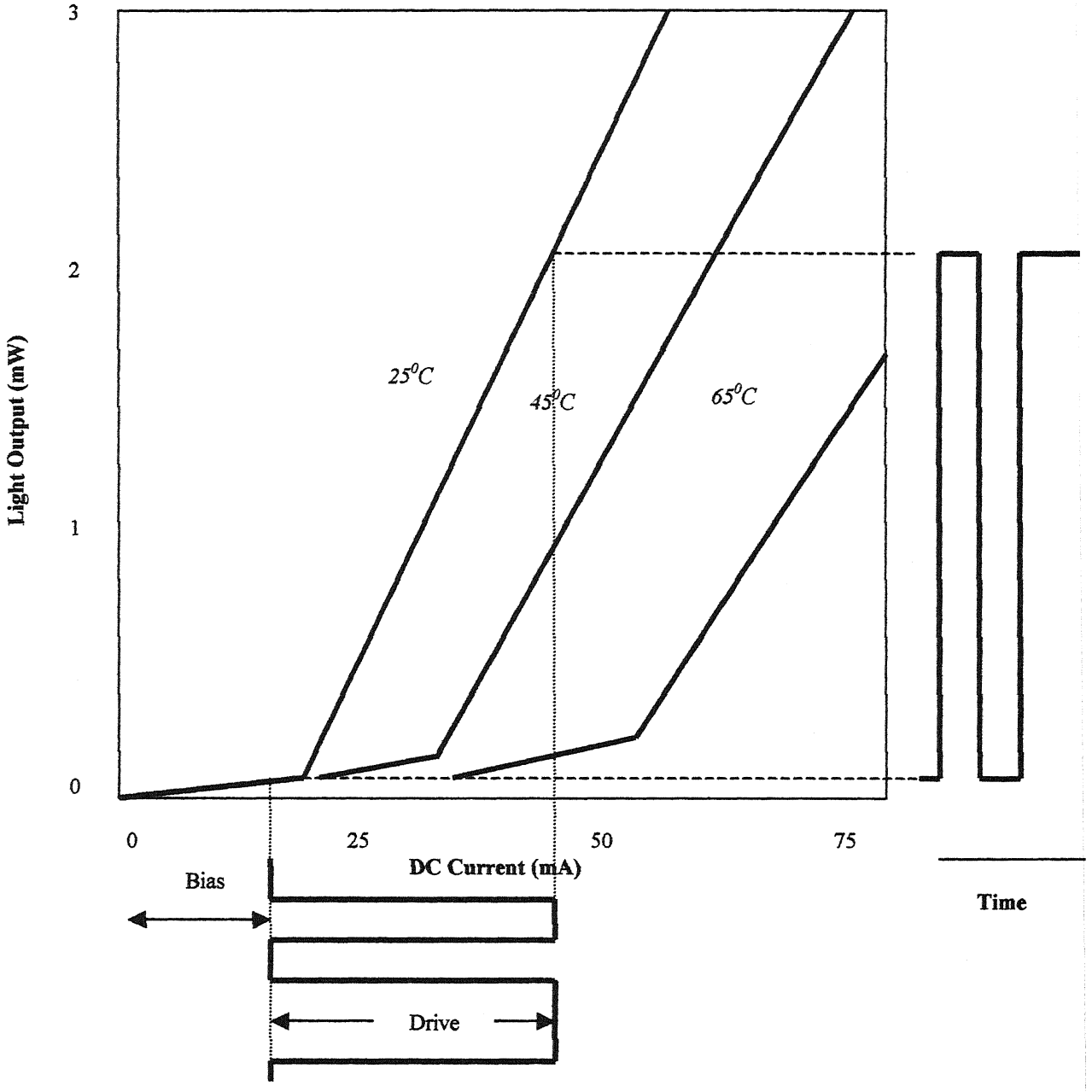

Fig. 2.5. Transfer characteristics for typical high speed pulsed operation of a laser.

with respect to threshold, in which case Equation 2.2 becomes

$$t_d = \tau_{th} \ln \frac{I}{I-(I_{th}-I_{bias})} \quad \ldots\ldots\ldots\ldots\ldots\ldots\ldots\ldots\ldots\ldots\ldots\ldots\ldots\ldots\ldots \text{(2.3)}$$

It is seen that the delay vanishes when $I_{bias}=I_{th}$. The amplitude of the overshoot or ringing (whose frequency is nearly equal to the laser resonance frequency and whose damping time constant is twice the recombination lifetime), becomes small as the laser is biased near threshold. Therefore, to minimize delay and overshoot, both of which cause serious pattern dependant distortion, a near threshold dc bias is added to the pulse current, resulting in an operation as shown in Fig. 2.5. [3].

This bias, however results in a nonzero '0' light level, reducing the extinction ratio and incurring a sensitivity penalty at the receiver. Therefore the bias current used must be optimum for the application in mind and chosen carefully. Also to be considered is the transmitter circuit's capability of maintaining this bias at the optimum point under all operating conditions.

Two other significant changes in laser characteristics may occur: These are the changes in the **mode spectra** (lasing wavelength, far field pattern, spectral width) and **self sustained oscillations** in the laser output. These may not be accompanied by decreased power (at constant current) or an increase in the threshold current.

2.2.3 TRANSMITTER CIRCUITS

Based on the discussions above, digital transmitter circuits should: -

(a) supply high-speed current pulses

(b) supply dc bias

(c) maintain high extinction ratio

(d) maintain constant output power

(e) provide laser protection

A block diagram of such a transmitter is shown in Fig. 2.6. [1]. The high-speed driver shown here is simply summed with the dc bias at a tee. Laser output is

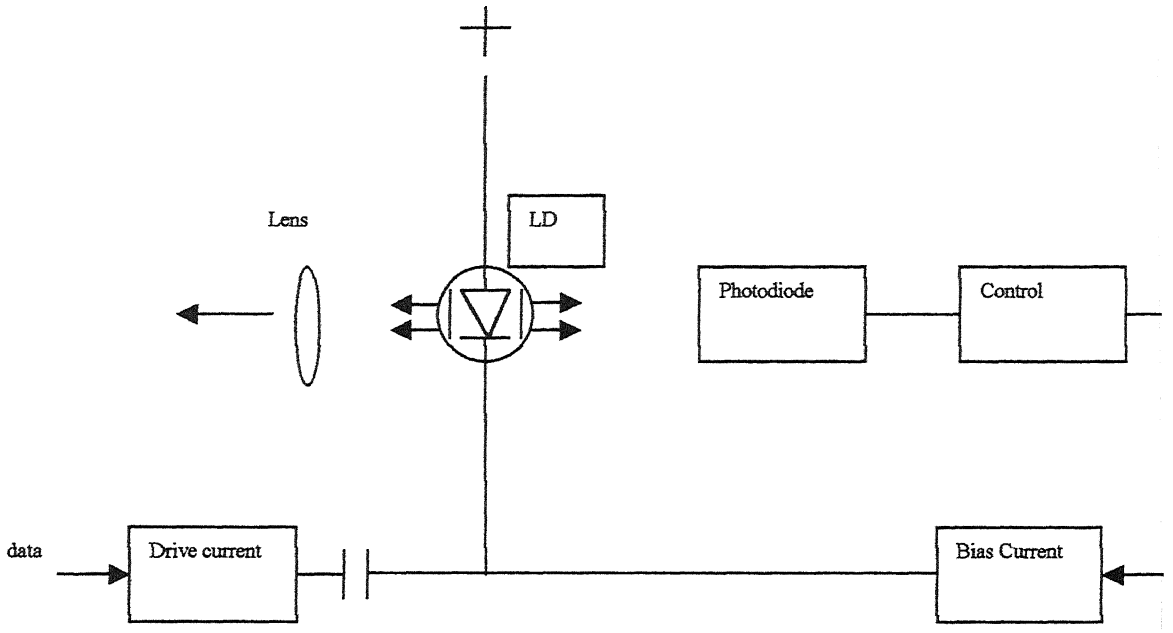

Fig. 2.6. Block diagram of directly modulated laser transmitter

monitored by the light emitted from the back mirror. The resulting photocurrent is used with a regulator circuit from which the bias is derived to maintain a constant output power.

A simple laser drive circuit for digital transmission is shown in Fig. 2.7. This circuit is a shunt driver utilizing an FET to provide high-speed laser operation. Sufficient voltage is maintained in series with the laser using the resistor R_2 and the compensating capacitor C such that the FET is biased into its active or pinch-off region. Hence for a particular input voltage V_{in} (i.e. V_{GS}) a specific amount of the total current flowing through $R_1$is diverted around the laser leaving the balance of the current to flow through R_2 and provide the off state for the device. Using stable gallium arsenide MESFETs the circuit has modulated lasers at rates in excess of 1Gbits/s.

An alternative high-speed laser drive circuit employing bipolar transistors is shown in Fig. 2.8. [1]. This circuit configuration consists of two differential amplifiers connected in parallel. The input stage, which is ECL compatible, exhibits a 50 Ω input impedance by using an emitter follower T_1 and a 50 Ω resistor in parallel with the input.

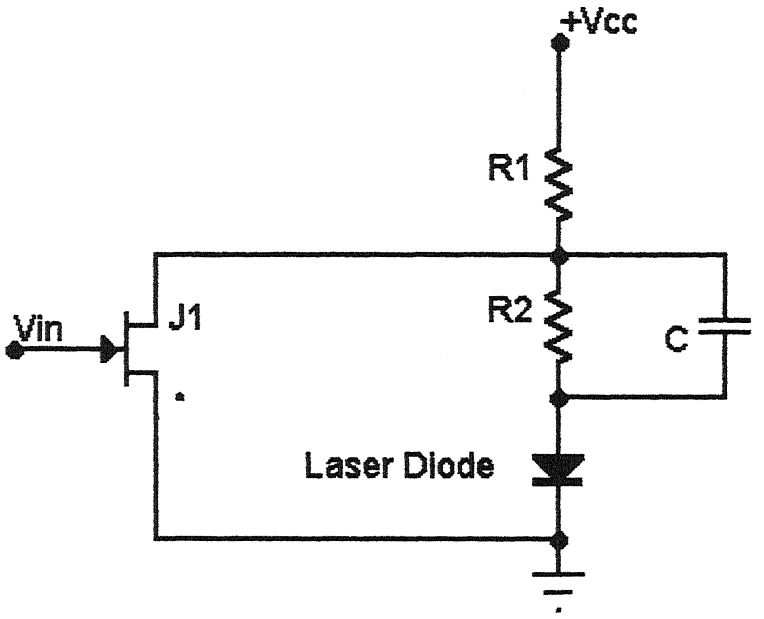

Fig. 2.7. A shunt drive circuit for use with an injection laser.

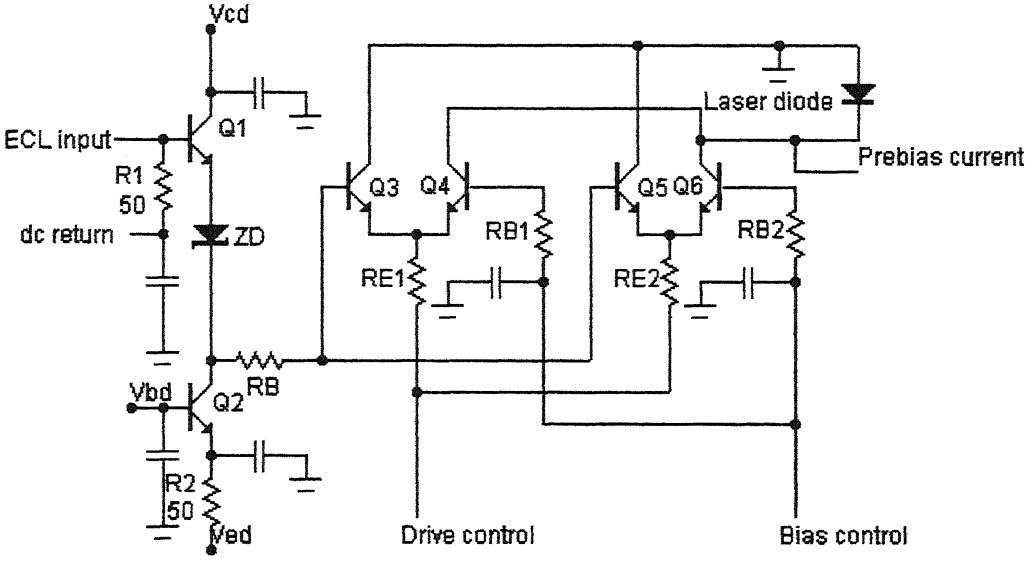

Fig. 2.8. An ECL compatible high speed laser drive circuit.

The transistor T_2 acts as a current source with the zener diode (ZD) adjusting the signal level for ECL operation. The two differential amplifiers provide sufficient modulation current amplitude for the laser under the control of a dc control current I_E through the emitter resistors R_{E1} and R_{E2}; I_E is provided by an optical feedback control circuit. A prebias current is applied to the laser from a separate current source. This circuit when utilizing microwave transistors was operated with a return to zero digital format at 1 Gbit/s.

2.3 THE RECEIVER

The optical receiver is a critical element of an optical communicating system since it often determines the overall system performance.

2.3.1 SYSTEM REQUIREMENT

The receiver terminal equipment will essentially consist of an **optical detector** which converts the received optical signal into an electrical current, **a pre-amplifier** where initial amplification is performed without additional noise corrupting the received signal, **a post amplifier** for providing additional low noise amplification of the signal, **an equalizer** for compensating the distorted input signal and to provide suitable signal shape, and a **filter** to maximize the received signal to noise ratio while preserving the essential features of the signal. A block schematic of the receiver showing the major elements is shown in Fig. 2.9.

The fundamental goal in the design of an optical receiver is to minimize the amount of optical power which must reach the receiver in order to achieve a given bit error rate (BER) in digital systems or a given signal to noise ratio (SNR) in an analog system. This power, commonly referred to as the sensitivity, and usually measured in dBm of optical power, depends upon the detector type and characteristics-either p-i-n or avalanche photodiode-as well as the pre-amplifier.

2.3.2 RECEIVER CIRCUITS

The input optical power required at the receiver depends on the detector type and the electrical components within the receiver structure. It is strongly dependent upon the

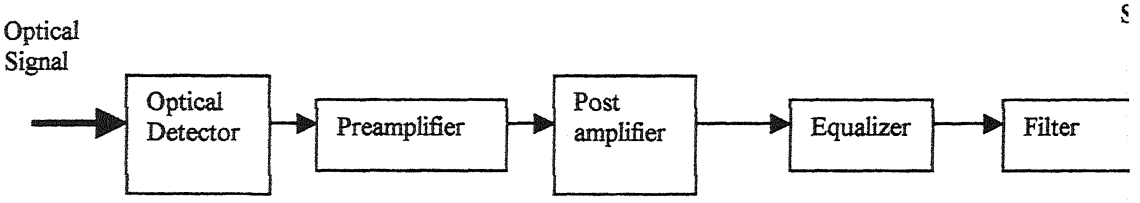

Fig. 2.9. Block schematic of a receiver.

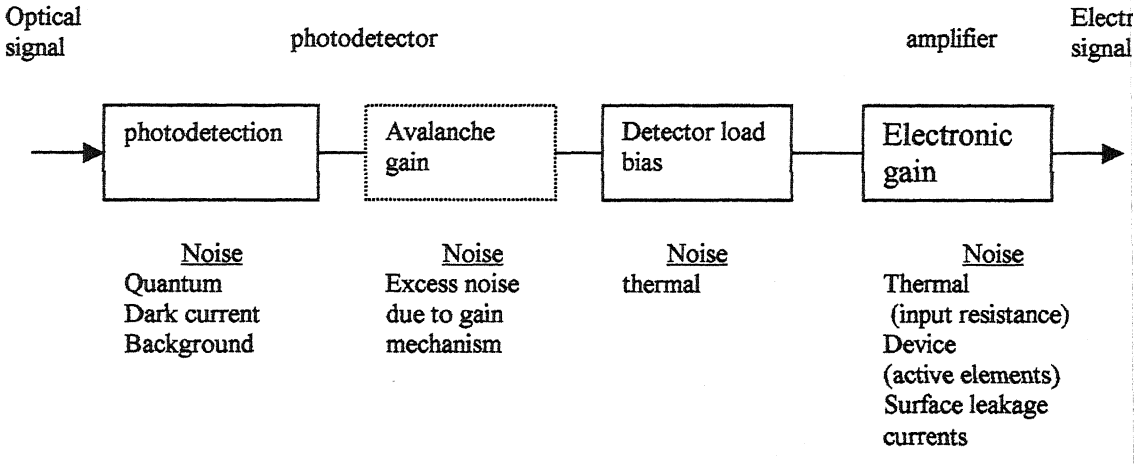

Fig. 2.10. Block schematic of the front end of an optical receiver showing the various sources of noise.

noise (i.e. quantum, dark, and thermal) associated with the receiver. Fig. 2.10. shows a block schematic of the front end (detector and pre-amplifier) of an optical receiver and the various noise sources associated with it [1].

There are basically three types of receiver front-end configurations, viz. low impedance, high impedance, and transimpedance front ends. Each one has its own merits and demerits. Selection of a front end depends upon the requirements of sensitivity, bandwidth and dynamic range. **Sensitivity** is defined as the minimum average optical power required at the receiver for a specified performance and data rate. **Dynamic range** specifies the range of power over which the receiver is able to function as per specifications. It is generally expressed in decibels as the ratio of the maximum optical power to the minimum optical power incident on the receiver giving the specified performance.

Low impedance front end: This type of front end is the simplest one where a very low resistance, of the order of 50 or 100 ohms, is used as the photodetector load resistance. The voltage developed across the low resistance is indeed the preamplifier output. This scheme has the advantage that the RC time constant is very small and hence this simple scheme can work up to very high frequencies. Its dynamic range is also very large. However, the low load resistance results in very large thermal noise and hence its sensitivity is very poor. This configuration is useful only when the optical signal levels are very large.

High impedance front end: This type of receiver also uses an open loop approach and has a very simple configuration where the detector load resistance is made very large. Due to the large load impedance the bandwidth of this receiver is very low. Hence the preamplifier stage must be followed by an equalization stage to compensate the low pass behavior of the front end. This type of front end has the advantage that the thermal noise generated by the load is very low. However, its dynamic range is very low because of the overloading due to large impedance. Due to its poor dynamic range and bandwidth, this type of receiver front end is used only when noise performance is the main criterion.

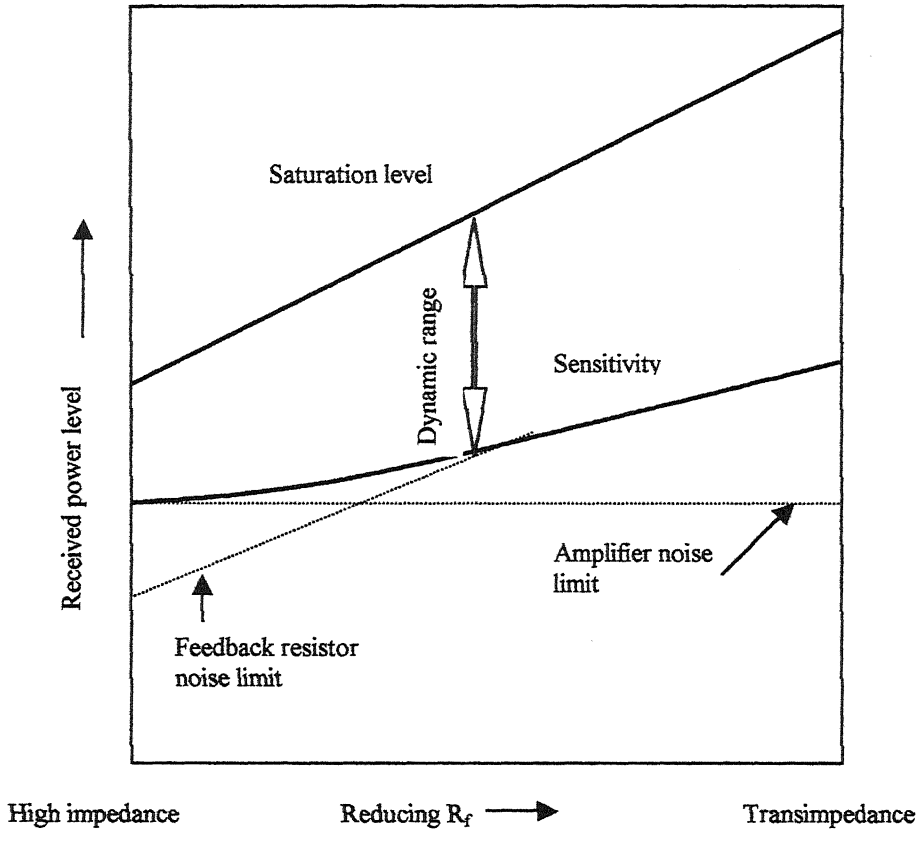

Fig. 2.11. Characteristics illustrating the variation in received power level against the value of the feedback resistor R_f

Transimpedance front end: This configuration largely overcomes the drawbacks of the high impedance front end by utilizing a low noise, high input impedance amplifier with negative feedback. No equalizing circuitry is required. However, because of the thermal noise of the feedback resistor, the receiver noise level is higher and the receiver sensitivity is somewhat less than that of a high impedance design. In principle, this receiver sensitivity degradation can be kept to negligible value by keeping the feedback resistance as large as possible. For a desired bandwidth value, this can be achieved by increasing the amplifier open-loop gain. Characteristics illustrating

the variation in received power level against the value of the feedback resistor R_f is shown in Fig. 2.11[1].

2.3.3 INTEGRATED OPTICAL RECEIVERS

Monolithic integration of several or many optical and electronic components on a single GaAs or InP chip has been an attractive technical goal for some time, as it may offer the same rewards of low-cost mass production and reliability of complex assemblies that have been achieved with silicon microelectronic circuits. Furthermore there are the inherent advantages of small physical size and low parasitic impedances that are very important for high-performance systems operating at very high frequencies. Integrated optical receivers comprising both photodetector and preamplifier stages are now advancing into the multi-gigabit per second regime, with emphasis ranging from completely monolithic to flip-chip mounted detector structures. Some of them are given below.

p-i-n/FET: An integrated PIN/FET optical receiver, consisting of a low capacitance InGaAs PIN photodiode, connected to a high impedance three stage GaAs FET preamplifier, fabricated as a thin film hybrid integrated circuit, has reported a bandwidth of 10 Gbit/s in the direct detection mode [12].

p-i-n/MESFETs: - This is fabricated by the integration of GaAs PIN photodetectors with amplifier circuits composed of GaAs MESFETs (metal semiconductor FET). These components are fabricated on a GaAs substrate with epitaxial layers grown by metal-organic chemical vapour deposition (MOCVD). It is reported that a transmission rate of 400 Mbit/s has been achieved with a bit error rate of 10^{-9} for received power of –18 dBm [3].

p-i-n/HBT: - In the past few years p-i-n diodes have been monolithically integrated with trans-impedance amplifiers employing hetrojunction bipolar transistors (HBTs) [16]. The advantage of using HBTs instead of FETs or homo junction bipolar transistors in high frequency optoelectronic circuits stem from:

(a) the freedom to lower the emitter doping concentration, thus lowering the base-emitter depletion capacitance, without lowering β.

(b) lower base transit times due to controlled vertical growth and possible ballistic transport.

UTC/HEMT: An OEIC receiver with a measured sensitivity of -27.5dBm for a 40 Gbit/s return to zero optical signal has been reported [9]. This consists of a monolithically integrated digital IC composed of a unitravelling carrier-photodiode (UTC-PD) directly connected to an InP HEMT (High Electron Mobility Transistor). The epitaxial layer structure of the OEIC was grown by MOCVD on semi-insulating InP substrates.

p-i-n/HEMT: Two fully integrated GaAs based OEIC photo receivers, one designed for wireless broadcast applications at 42GHz and another one for wireless local area networks operating at 60GHz has been reported [11]. Both receivers use a 1.3-1.55 μm wavelength $In_{0.53}Ga_{0.47}As$ p-i-n PD, grown lattice relaxed on GaAs, which is conjugately matched to a two stage monolithic microwave integrated circuit (MMIC) amplifier based on 0.15 μm GaAs based dual gate PHEMTs. The responsivity obtained were 7 A/W and 2.5 A/W, respectively.

Wave guide photodiodes (WGPDs) and Evanescently coupled photodiodes (ECPDs): Optical receivers in 40 Gbit/s optical transmission systems require fast and efficient photodiodes able to operate at high power levels. Although WGPDs are suitable for such high-speed applications, high power inputs of several milliwatts cause damage to the input facet of the photodetectors due to absorption of input light. ECPDs are much more robust than conventional WGPDs under high power input conditions due to the lower optical intensity in the absorption layer, although the quantum efficiency is relatively low. ECPDs with a high external efficiency of 0.71 A/W, obtained as a result of graded index configuration of the waveguide, have been developed. A bandwidth in excess of 40GHz has been reported up to an average photocurrent of 10mA [10].

2.4 OPTICAL SYSTEMS

Optical wireless receivers differ from their fiber optic counterparts in two significant ways. First, the dominant source of shot noise in fiber optic receivers either arises from the signal itself or the dark current in the detector. In an optical wireless receiver, by far the dominant source of shot noise in the detector arises from the ambient light levels in the environment, necessitating the use of *optical filters* in many applications. Secondly, in a fiber optic receiver, the optical power is received as a concentrated beam permitting the use of extremely small detectors. By contrast, in an optical wireless receiver, large area photodiodes are required to capture as much of the signal as possible. Increasing the photodiode area is expensive, and tends to decrease receiver bandwidth due to the large capacitances associated with such detectors and increase receiver noise. Hence it is desirable to employ an *optical concentrator* to increase the effective area.

2.4.1 OPTICAL FILTERS

Optical wireless receivers typically employ either longpass or bandpass optical filters to attenuate ambient light. Longpass filters can be thought of as essentially passing light at all wavelengths beyond the cutoff wavelengths and are usually constructed of colored glass or plastic, so that their transmission characteristics are substantially independent of the angle of incidence. Bandpass filters are usually constructed of multiple thin dielectric films as shown in Fig. 2.12., and rely upon the phenomenon of optical interference. These filters can achieve narrow bandwidths, leading to superior ambient light rejection. The basic component of a thin film filter is the Fabry-Perot resonator, with the mirrors replaced by distributed reflectors consisting of a stack of alternating high and low index dielectrics, each a quarter wave thick, which essentially acts as a comb-line filter. For optical bandwidths of $\leq$100 nm, required in optical wireless applications, two or more resonator sections are coupled together.

2.4.2 OPTICAL CONCENTRATORS

The purpose of an optical concentrator is to transform light rays incident over a wide area into a set of rays that emerge from a smaller area. In optical wireless

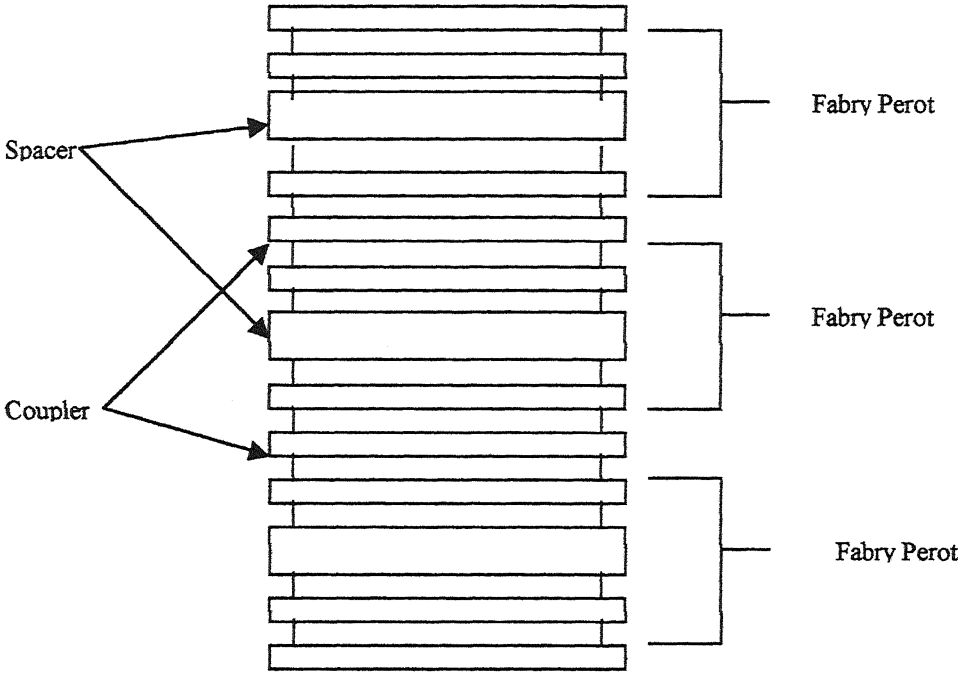

Fig. 2.12. Schematic of a thin film optical filter.

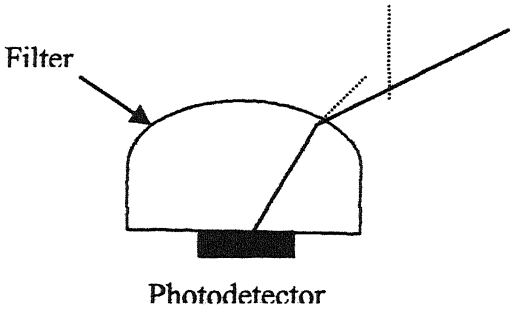

Fig. 2.13. Nonimaging optical concentrator.

applications, concentrators are typically employed to improve the collection efficiency at the receiver. Concentrators may be either imaging or nonimaging. The telescope used in long range, free space optical links represent examples of imaging concentrators. Most short-range infrared links employ nonimaging concentrators. Fig 2.13 shows a nonimaging optical concentrator.

2.4.3 OPTICAL AMPLIFIERS

Optical amplifiers as their name implies, operate solely in the optical domain with no conversion of photons to electrons and can be used as a single in-line component for any kind of modulation at virtually any transmission rate. They may also be used as optical receiver preamplifiers, linear repeaters, optical gain blocks, optical gates, pulse shapers and routing switches. The two main approaches to optical amplification to date have concentrated on semiconductor laser amplifiers and fiber amplifiers. In semiconductor laser amplifiers gain is provided by stimulated emission from injected carriers whereas in fiber amplifiers it is by stimulated Raman scattering or by rare earth dopants [1]. Both types have the ability to provide high gain (5-20dB) over a wide spectral bandwidths (1.46-1.62μm). The majority of today's developmental work on amplifiers is devoted to the erbium doped fiber amplifier (EDFA) variety as they can readily realize the features crucial to high performance transmission systems.

2.5 FREE SPACE MEDIUM

The primary disadvantage of free space laser communication was mentioned earlier as its vulnerability to atmospheric effects, which can reduce link availability and may introduce burst errors. Atmospheric effects can be broken down into two broad categories: losses due to atmospheric attenuation and losses due to atmospheric turbulence or scintillation.

2.5.1 ATMOSPHERIC ATTENUATION

Attenuation consists of absorption and scattering of the laser light photons by the different aerosols and gaseous molecules in the atmosphere. It is described by Beer's law as [13]

$$\tau(R) = \frac{P(R)}{P(0)} = e^{-\sigma R}, \quad (2.4)$$

where $\tau(R)$ = transmittance at range R,

$P(R)$ = laser power at R,

$P(0)$ = laser power at the source,

σ = attenuation coefficient

The attenuation coefficient is made up of four parts: $\sigma = \alpha_m + \alpha_a + \beta_m + \beta_a$,

where α_m = molecular absorption coefficient,

α_a =aerosol absorption coefficient,

β_m = molecular or Rayleigh scattering coefficient,

β_a = aerosol or Mie scattering coefficient.

Aerosols include finely dispersed solid and liquid particles, such as water droplets, ice, dust, and organic materials. They vary in size from a few molecules to 20μm in radius. The important atmospheric molecules that have high absorption in the IR band include water, CO_2 , ozone, and O_2. There are transmittance windows in the absorption spectra for these atmospheric molecules.

2.5.2 ATMOSPHERIC TURBULENCE

Occasional burst errors of the order of 1 ms or less occur during laser communication transmission primarily due to small-scale dynamic variation in the index of refraction of the atmosphere. Atmospheric turbulence (i.e. wind) produces temporary pockets of air with slightly different temperatures, different densities, and thus different indices of refraction. These air pockets are continuously being created and then destroyed as they are mixed. Data can be lost due to *beam wander* and *scintillation* as the laser beam becomes deformed propagating through these index of refraction inhomogeneities. The significance of each effect depends on the size of these turbulence cells with respect to the laser beam diameter. If the size of the turbulence cells is larger than the beam diameter, the laser beam as a whole randomly bends, causing possible signal loss if the beam wanders off the receiver aperture. More commonly, if the size of the turbulence cells is smaller than the laser beam diameter, ray bending and diffraction causes distortion in the laser beam wave front. Small variations in the arrival time of various

components of the beam front produce constructive and destructive interference, and results in temporal fluctuations in the laser beam intensity at the receiver. The fluctuations in the receive power are similar to the twinkling of a distant star, hence called *scintillation.* The constant mixing of the atmosphere produces unpredictable turbulent cells of all sizes, resulting in received signal strength fluctuations that are a combination of *beam wander* and *scintillation.* Scintillation fluctuations occur on a time scale comparable to the time it takes these cells to move across the beam path due to the wind. Scintillation fluctuations can be reduced by using either multiple transmit beams or a large receive aperture.

2.6 EYE SAFETY CONSIDERATIONS

Optical wireless systems like their radio counterparts, can pose a hazard if operated incorrectly. Therefore a laser safety standard has been established in which optical sources has been classified in accordance with their total emitted power. The principal classifications are summarized in Table 2.1. for a point source emitter such as a semiconductor laser[15].

Out door point-to-point systems, generally use high power lasers that operate in the class 3B band to achieve a good power budget. The safety standard recommends that these systems should be located where the beam cannot be interrupted or viewed inadvertently by a person. Roof top locations or high walls are usual for this type of systems.

The wavelength band between about 780 and 950 nm is presently the best choice for most applications of infrared wireless links, due to the availability of low cost LEDs and laser diodes (LDs), and because it coincides with the peak responsivity of inexpensive, low capacitance Si photodiodes. The primary draw back of radiation in this band relates to eye safety: it can pass through the human cornea and be focused by the lens on to the retina, where it can potentially induce thermal damage. The cornea is opaque to radiations beyond 1400nm, considerably reducing potential ocular hazards, so that it has been suggested that the 1550 nm band may be better suited for infrared links.

Wave Length	650 nm	880 nm	1310nm	1550 nm
Class 1	Up to 0.2 mW	Up to 0.5 mW	Up to 8.8 mW	Up to 10 mW
Class 2	0.2-1 mW	N/A	N/A	N/A
Class 3A	1-5 mW	0.5-2.5 mW	8.8-45 mW	10-50 mW
Class 3B	5-500 mW	2.5-500 mW	45-500 mW	50-500 mW

Table. 2.1. Laser safety classifications for a point source emitter.

SYSTEMS	TerraLink Laser Commn. Systems	Cable-free Gigabit-1000 link	BT labs	Terescope Free Space Optics	ITCOM WP5100
DETECTOR	APD/PIN	N/A	1mm Si APD with narrow band interference filter	N/A	FID3ZILXF Photodiode Fujitsu make
SOURCE	Laser diode of average power 20mW, wavelength 780/825 nm	Laser	GaAs/GaAlAs Fabry-Perot Laser of wavelength 820 nm	Laser with multiple transmit aperture technology	FLD5F8LK Laser of Fujitsu of average power 0.8 mW, 1550 nm
BIT RATE (Mbps)	230/622	2.048	1000	155	4000
DISTANCE (km)	8/3.5	0.35	0.04	3.75	N/A
BER	10^{-9}	10^{-9}	10^{-9}	10^{-9}	10^{-9}
REFERENCE	[13]	[19]	[18]	[20]	[21]

Table 2.2. Comparison of various out door infrared systems.

Unfortunately, the photodiodes presently available for this band, which are made of germanium or InGaAs, have much higher costs and capacitances per unit than their Si counterparts. At present, most of the commercially available systems operate in the shorter wavelength band.

2.7 COMPARISON OF VARIOUS SYSTEMS

Table 2.2. gives a comparison of some of the outdoor optical wireless systems reported so far on the basis of their features.

CHAPTER 3

DESIGN OF AN OUTDOOR HIGH-SPEED OPTICAL WIRELESS LINK

Before any system design procedures can be initiated, it is essential that certain basic system specifications be laid down. The system specifications for our outdoor optical wireless link were as follows:

Required transmission data rate	:	40 Mbps
Distance between terminal equipment:		> 40m
Transmission type	:	Digital
Acceptable system BER	:	10^{-9}
Cost	:	moderate
Reliability	:	High.

The system designer has many choices when selecting components for an outdoor optical communication system. In order to exclude certain components at the outset it is useful if the operating wavelength of the system is established (i.e. shorter wavelength region 0.8-0.9 μm or larger wavelength region 1.1-1.6 μm). This decision will largely be dictated by the overall requirements for the system performance, the ready availability of suitable reliable components and cost. The major components are:

a) **Source type and characteristics:** Laser or LED; optical power launched into the medium, rise and fall time, stability etc.

b) **Transmitter configuration:** Digital or analog transmission; input impedance, supply voltage, dynamic range, optical feedback etc.

c) **Detector type and characteristics:** p-n, p-i-n, or avalanche photodiode; responsivity, response time, active diameter, bias voltage, dark current etc.

d) **Receiver configuration:** Preamplifier design (low impedance, high impedance or trans-impedance front-end), BER or SNR, dynamic range etc.

e) **Modulation and coding:** Source intensity modulation, using pulse modulation techniques for either digital (e.g. PCM, Adaptive delta modulation) or analog (PAM, pulse frequency modulation, PWM, PPM) transmission. Also encoding schemes for digital transmission such as biphase (Manchester) and delay modulation (Miller) codes. Alternatively analog transmission using direct intensity modulation or frequency of the electrical sub-carrier.

3.1 RECEIVER DESIGN

In the design of an outdoor optical wireless link, one of the key elements of the system is the receiver. The basic purpose of the receiver is to detect the light incident upon it and to convert it to an electrical signal containing the information impressed on the light at the transmitting end. It basically consists of a photodetector, a preamplifier, a post amplifier, a comparator and a driver stage as shown in Fig. 3.1.

3.1.1 SPECIFICATIONS FOR THE RECEIVER

Keeping in mind the overall system specifications laid down, the receiver specifications were formulated based on the important receiver characteristics like *bandwidth, sensitivity, dynamic range* and criteria like *reliability, simplicity of circuit, stability* and *cost.*

Bandwidth of the receiver should be at least 20 MHz to be able to receive a bit rate of 40 Mbps as per Nyquist criteria. If a pessimistic approach is taken the receiver bandwidth should be 40 MHz. But since this is a point-to-point outdoor link the transmitter power can be up to several milliwatts and also the full transmitter power is concentrated on to the receiver. Hence a bandwidth of about 30 MHz for the receiver should be a safe choice.

For a point-to-point link, once installed the *dynamic range* requirement is not very stringent. It has to cater only for environmental and ageing margins and the range of link

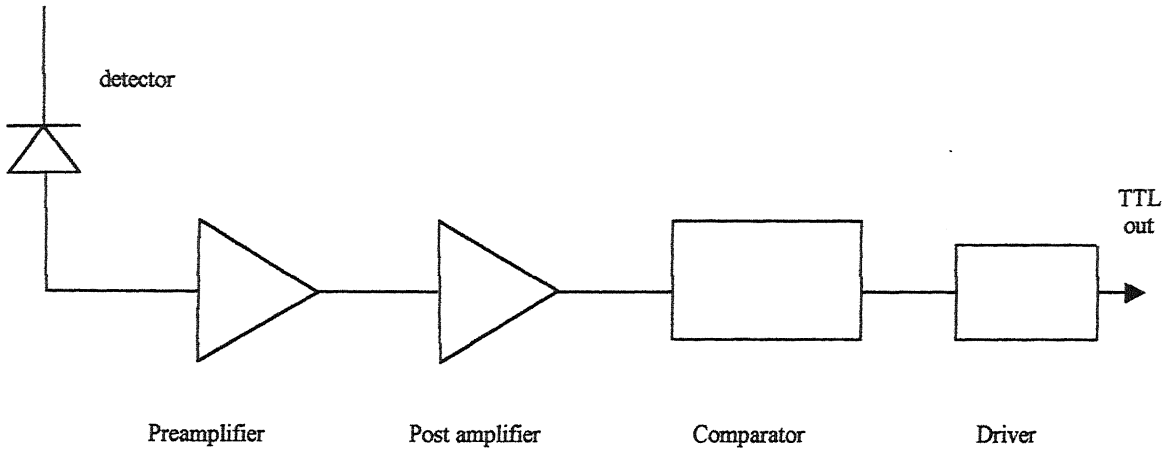

Fig. 3.1. Schematic of an optical receiver

Bit rate	>40 Mbps
Dynamic range	>15 dB
Sensitivity	Better than –28.9 dBm
Cost	Moderate
Reliability	High
Circuit complexity	Simple
Time for design and fabrication	3 months

Table 3.1. Summary of specifications for the optical receiver.

length that the receiver is expected to accommodate. Since the range to be achieved is specified as >40m and no upper limit is specified, we can safely set the dynamic range to be > 15 dB of optical power [7].

As far as the *sensitivity* of the receiver is concerned, one always tries to make the most sensitive receiver. But considering limitations set by the quantum limit and compromises required in a practical receiver due to various factors like dynamic range, thermal noise, dark current, inter symbol interferences and degradation due to the optical source, a practical receiver can achieve around 10-15dB of the fundamental limit set by the quantum theory, which is –38.9dBm for a p-i-n diode [7,22]. So for a 40 Mbps bit rate receiver, using p-i-n detector operating in the shorter wavelength of 0.8-0.9 μm, one can achieve sensitivity in the range of –28.9 dBm to –23.9 dBm, for a BER of 10^{-9}.

The *cost* should be as little as possible using components available in the laboratory and the circuit should be simple, reliable and stable. Time allotted for this work was 3 months for design and implementation. The summary of specifications for the optical receiver is given in Table 3.1.

3.1.2 CHOICE OF RECEIVER ELEMENTS

The fundamental goal in the design of an optical receiver is to minimize the amount of optical power that must reach the receiver in order to achieve a given BER or SNR. This power commonly referred to as sensitivity, depends upon the detector type and characteristics as well as the design of the amplifier.

3.1.2.1 Optical Detectors

An optical detector is an optoelectronic device that absorbs optical energy and converts it into electrical energy. There are generally three steps involved in this process:

a) Absorption of optical energy and generation of carriers
b) Transportation of the photogenerated carriers across the absorption region
c) Carrier collection and generation of a photocurrent

The following criteria define the important performance and compatibility requirements for detectors:

a) High sensitivity at the operating wavelengths. The first generation systems have wavelengths between 0.8 and 0.9 μm compatible with AlGaAs laser and LEDs.

b) High fidelity to reproduce the received signal waveform with fidelity over a wide range.

c) Large electrical response to the received optical signal. The photodetector should produce a maximum electrical signal for a given amount of optical power i.e. the quantum efficiency should be high.

d) Short response time to obtain a suitable bandwidth as future systems will operate in the gigahertz range and above.

e) A minimum noise introduced by the detector. Dark currents, leakage currents and shunt conductance should be low. Also the gain mechanism within either the detector or associated circuitry must be of low noise.

f) Stability of performance characteristics. Ideally the performance characteristics of the detector should be independent of the changes in ambient conditions. However, detectors currently favoured (photodiodes) have characteristics (sensitivity, noise, internal gain), which vary with temperature, and therefore compensation for temperature effects is often necessary.

g) Low bias voltages. Ideally the detector should not require excessive bias voltages or currents.

h) High reliability. The detector must be capable of continuous stable operation at room temperature for many years.

j) Low cost. Economic considerations are often of prime importance in any large-scale communication system application.

The three main types of detectors are photoconductors, PIN diodes, and avalanche photodiodes. PIN photodiodes have no internal gain but can have very large bandwidths. Detectors are also classified into intrinsic and extrinsic types. An intrinsic photodetector usually detects light of wavelength close to the bandgap of the semiconductor, whereas an extrinsic photodetector detects light of energy smaller than the bandgap energy. With intrinsic absorption, the received photons excite electrons from the valance to the

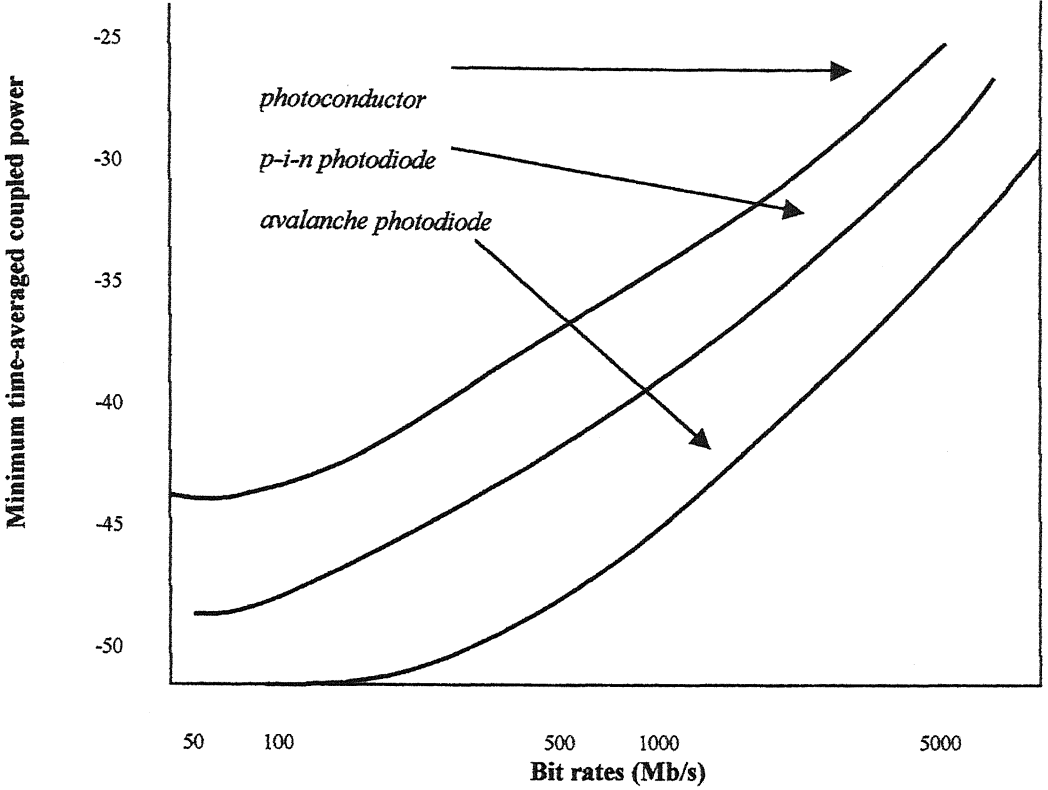

Fig. 3.2. Minimum detectable power as a function of bit rates for the three types of detectors used in optical communication.

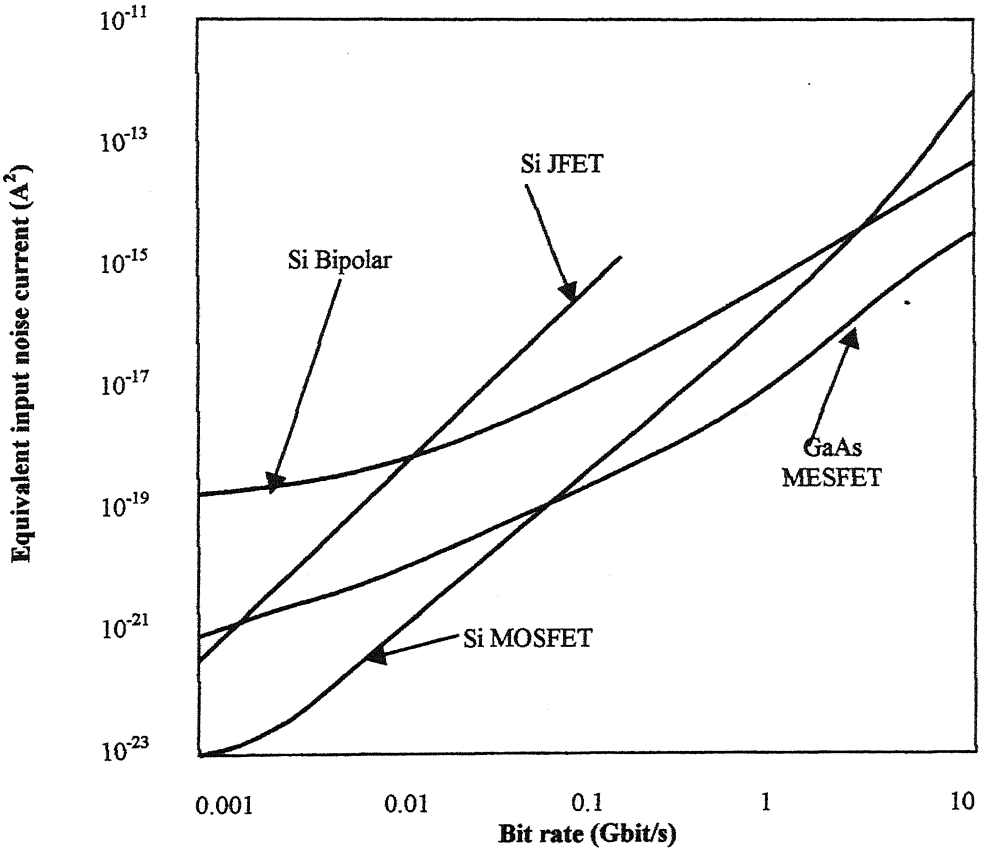

Fig. 3.3. Noise characteristics for various optical receivers

conduction bands in the semiconductor, whereas extrinsic absorption involves impurity centres created within the material. However, for fast response coupled with efficient absorption of photons, the intrinsic absorption process is preferred.

The application usually decides the detector of choice. A useful figure of merit is the minimum detectable time averaged signal power. A photoconductor is an attractive device, considering its simplicity of fabrication and ease of operation. However, its high dark current and the associated Johnson noise make it unsuitable for high-performance communication applications. The best combination of bandwidth and sensitivity is obtained by the p-i-n diode and the APD. Fig. 3.2. shows a comparison of the minimum detectable optical power in photoconductors, p-i-n diodes and APDs [1].

Avalanche photodiodes are advantageous over PIN photodiodes in applications where electrical noise in the preamplifier is dominant, and not the shot noise. They enjoy great success in systems where the signal itself is weak, and the only source of noise is the shot noise of the photodetector dark current. In optical wireless systems, however, the background light is generally large resulting in high shot noise, even with PIN diode, thus limiting the usefulness of APDs. Hence we decided to use a PIN photodiode as the detector.

3.1.2.2 FET vs. BJT for the Front-end : The amplifier device having the lowest noise, and widely available, is the silicon FET. Unlike the BJT, the FET has extremely high input impedance, low noise and low capacitance, which make the FET, appear as an ideal choice for the front end. However it has a very low transconductance. Hence at low bit rates the FET is superior whereas at higher bit rates (>50MHz) the bipolar devices produce superior performance. Fig. 3.3. shows the noise performance of various preamplifiers over a range of bandwidths [2].

Since the transmission bandwidth requirement of our system was only 30 MHz, we decided to use an FET as front-end amplifier device.

3.1.3 RECEIVER DESIGN

Of most importance to the optical receiver are the photodetector and the following low noise preamplifier. Together these two elements dictate many of the receiver's

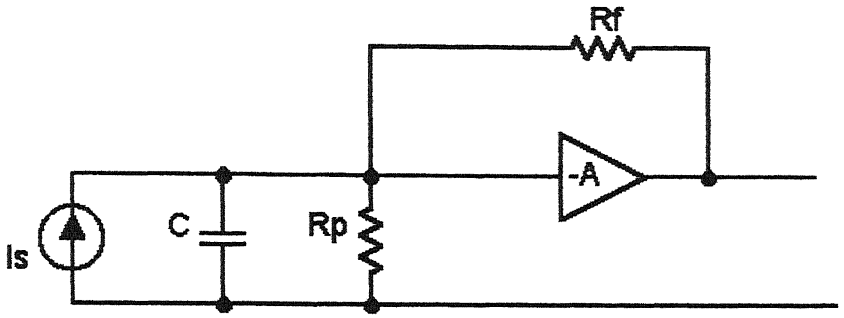

Fig. 3.4. Feed back(TZ) amplifier.

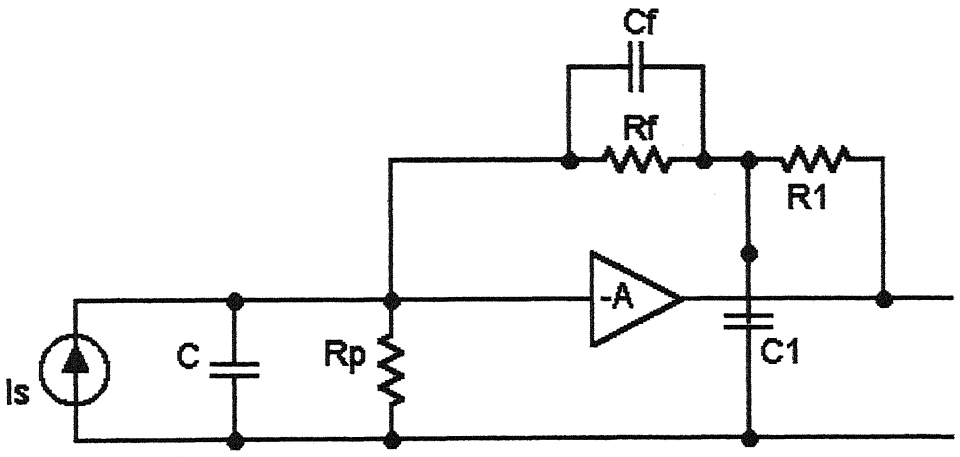

Fig. 3.5. Feed back amplifier with compensating network.

characteristics as well as its performance. We decided to choose the popular transimpedance (TZ) preamplifier design with a FET front end [7]. TZ amplifier is shown in Fig. 3.4.

The TZ preamplifier design is a popular approach to avoid the dynamic range problem. In addition, it is normally designed to take advantage of the negative feedback effect so that the amplifier bandwidth is extended to the desired value. Thus no equalizing circuitry is required. However because of the thermal noise of the feedback resistor, the receiver noise level is higher and the receiver sensitivity is somewhat less than that of a high impedance design.

In principle, the receiver sensitivity degradation of the transimpedance design can be kept to negligible value by keeping the feedback resistance as large as possible. For a desired bandwidth value this can be achieved by increasing the amplifier open-loop gain. However the maximum open loop gain is ultimately limited by the propagation delay and phase shift of the amplifying stages inside the feed back loop. A certain gain and phase margin is desirable to assure stability and acceptable pulse response. Thus as the bit rate increases, the number of amplifying stages and the open loop gain is necessarily reduced. As a result the thermal noise of the feedback resistance in a transimpedance amplifier is normally a significant portion of the total noise.

It should be noted that a receiver amplifier can be designed to have transimpedance structure but with the feedback resistance increased so that its thermal noise contribution to the receiver noise is negligible. Such an amplifier is still classified as a high impedance design because it usually requires further equalization.

The receiver amplifier noise level is often characterized by an input equivalent noise current power $< i_{na}^2 >$ at a given operating bit rate. For a FET front-end amplifier, the input equivalent noise current power is given by [7]

$$< i_{na}^2 > = \frac{4kT}{R_f} I_2 B + 2eI_L I_2 B + \frac{4kT\Gamma}{g_m}(2\pi C_T)^2 f_c I_f B^2 + \frac{4kT\Gamma}{g_m}(2\pi C_T)^2 I_3 B^3 \quad \ldots\ldots(3.1)$$

where,

B --- operating bit rate,

R_f --- feedback resistance in TZ design,

I_L --- total leakage current (FET gate current and un-multiplied dark current component of the photodiode),

g_m --- FET transconductance,

C_T --- total input capacitance (including photodiode and stray capacitance),

f_c --- the 1/f noise corner frequency of the FET,

Γ --- numerical constant,

k --- Boltzman constant, and

T --- absolute temperature.

I_2, I_3 and I_f are weighting functions, which are dependent only on the input optical pulse shape to the receiver and the equalized output pulse shape. For NRZ coding format and the equalized out put pulse with a full raised cosine spectrum, we have $I_2 = 0.562$, $I_3 = 0.0868$ and $I_f = 0.184$. Parameter Γ is a noise factor associated with a channel thermal noise and a gate induced noise in the FET. It is normally taken to be 0.7 for Si FET's.

The total capacitance C_T is given by

$$C_T = C_{ds} + C_{gs} + C_{gd} + C_f \quad \text{.....(3.2)}$$

where,

C_{ds} = photodetector and stray capacitance at the input,

C_{gs} and C_{gd} = gate to source and gate to drain capacitance of the FET resp.,

C_f = stray capacitance of the feedback resistor.

In Equation 3.1, the first noise term is due to the feedback resistance, which is negligible if the HZ design is used. The second and third noise terms are contributions from the leakage current and 1/f noise. Finally, the fourth noise term is due to the channel thermal noise and induced gate noise. Equation 3.1 can be rewritten as follows:

$$\langle i_{na}^2 \rangle = \frac{4kT}{R_f} I_2 B + 2eI_L I_2 B + \frac{4kT\Gamma}{g_m}(2\pi C_T)^2 \left(1 + \frac{I_f f_c}{I_3 B}\right) I_3 B^3 \quad \text{.....(3.3)}$$

From this equation, we can see that it is desirable to choose an FET with a low gate leakage current, low input capacitance, high transconductance and low 1/f noise corner frequency.

Sensitivity: - The receiver sensitivity in terms of average detected optical power required at the receiver input for a desired error rate is given by [7]

$$\eta\ \bar{P} = Q\frac{h\Omega}{e}\left[QeBI_1F(G) + \sqrt{\frac{\langle i_{na}^2\rangle}{G^2} + 2eI_{dm}F(G)BI_2}\right] \quad \text{.....(3.4)}$$

where

η = photodetector quantum efficiency,

$\bar{P}$ = average optical power required for a desired BER

$h\Omega = hc/\lambda$, the photon energy,

Q = a parameter relating to the desired error rate (6 for BER of 10^{-9} [ ]),

For the case of a simple p-i-n photodiode, we have G = F(G) = 1 and $I_{dm} = 0$. In addition, the amplifier noise term $\sqrt{\langle i_{na}^2\rangle}$ normally dominates the signal shot noise term $QeBI_1$ in (3.4). Thus the receiver sensitivity expression for a p-i-n photodiode becomes

$$\eta\ \bar{P} = Q\frac{h\Omega}{e}\sqrt{\langle i_{na}^2\rangle} \quad \text{.....(3.5)}$$

Thus we see that for a p-i-n photodiode, the receiver sensitivity is proportional to $\sqrt{\langle i_{na}^2\rangle}$. The effect of dark current on the receiver sensitivity is such that, higher the bit rate, the less important the noise effect of the dark current. Other receiver sensitivity degradation sources are inter-symbol interference, optical source extinction ratio and optical source bandwidth.

Dynamic range: - The receiver dynamic range is the difference (in decibels) between the minimum detectable power level (receiver sensitivity) and the maximum allowable input power levels. As the received optical power increases, from its minimum level, the receiver bit error rate decreases because a higher signal to noise ratio is obtained. This improved performance continues until saturation or overloading occurs at the receiver. At this point (i.e. end of linear operation), the received signal waveform becomes distorted and the error rate starts to increase due to inter-symbol interference.

The dynamic range is a function of the feedback resistor of the front-end receiver amplifier. As the feedback resistor decreases, the maximum allowable received optical power increases. Thus the dynamic range is increased. However, reduction in the feedback resistor, results in an increase in the amplifier noise level. Thus there is a trade-off between high receiver sensitivity and wide dynamic range.

Bandwidth: - Let us now consider the current to voltage transfer functions of two amplifiers, one without feed back (HZ) and the other with feedback (TZ). For the non-feed back case this transfer function H(ω) is given by [23]

$$H(\omega) = \frac{AR_p}{1 + j\omega R_p C_T} \quad V/A \qquad \ldots\ldots(3.6)$$

where

A = open loop voltage gain

$R_p = \frac{R_b R_i}{R_b + R_i}$ and $C_T = C_d + C_i$

R_b = bias resistor,

R_i = input resistance of the amplifier,

C_d = detector capacitance,

C_i = input capacitance of the amplifier.

For the feedback case the transfer function $H_F(\omega)$ is,

$$H_F(\omega) = \frac{R_f}{1 + (j\omega R_f C_T / A)} \quad V/A \qquad \ldots\ldots(3.7)$$

Comparing Equation 3.6 and Equation 3.7 it can be seen that the feed back amplifier has a much greater bandwidth than the non-feedback amplifier, particularly if A is large. This greatly facilitates subsequent equalization and makes the feedback configuration, in the medium frequency range, most attractive from the design viewpoint. At high frequencies the propagation delay existing in the closed loop of the feedback amplifier reduces the phase margin and becomes a significant design factor.

A feedback amplifier is shown in simplified form in Fig. 3.4. From Equation 3.1 we see that a low output noise level requires the use of a high value of R_f and a small value of C_T. The amplifier however has a pole at an angular frequency of A/R_fC_T, so that by increasing R_f the bandwidth would be reduced necessitating more equalization. To overcome this one makes A as large as the stability of the closed loop will allow.

Another factor, which serves to reduce the amplifier bandwidth, is the stray capacitance that must necessarily be associated with the feedback resistor R_f. We denote this capacitance C_f. Taking C_f into account the closed loop response becomes [23]

$$H_F(\omega) = \frac{R_f}{1 + j\omega R_f\left(C_T/A + C_f\right)} \quad \ldots\ldots(3.8)$$

The usual means of cancelling the effect of C_f is to employ a compensating network as shown in Fig. 3.5. With this network the feedback factor β_F is [23]

$$\beta_F = \frac{1 + R_{fs}}{R_f + R_1 + (C_f + C_1)R_f R_{1s}} \quad \ldots\ldots(3.9)$$

with R_1 and C_1 being the elements of the compensating network. If $R_fC_f = R_1C_1$, the feedback factor becomes

$$\beta_F = \frac{1}{R_f + R_1} \quad \ldots\ldots(3.10)$$

With respect to the noise level, so long as $R_1 << R_f$, its contribution to the output noise is negligible.

Preamplifier design: - The design of the preamplifier requires particular attention since it may be expected to contribute most of the amplifier noise. The FET in the preamplifier stage is operated optimally in common source mode. In this mode the input impedance, the power gain and the out put impedance are high. In this case the input capacitance C_i comprises the parallel combination of the gate to source capacitance C_{gs} and the miller capacitance associated with the gate to drain capacitance C_{gd}. Therefore to minimize C_i one must overcome the miller effect by reducing the voltage gain of the FET. This can be achieved by following the common source stage with a stage having low input impedance. We decided to realize this using a shunt feedback stage using BJT, to ensure good bandwidth. The common source FET with shunt feedback stage is shown in Fig. 3.6.

Advantages of a shunt feed back stage are that it offers very good rejection of noise from succeeding stages without introducing more noise itself and also because of its low output impedance, reduces the effect of loading from the next stage.

3.2 TRANSMITTER DESIGN

The unique properties and the characteristics of the injection laser and the light emitting diode (LED), which make them attractive sources for optical transmission, were

discussed in the previous chapter. Keeping this in mind, and the system specifications laid down, the specifications for the transmitter were formulated.

3.2.1 SPECIFICATIONS FOR THE TRANSMITTER

For an outdoor high-speed wireless optical link, as specified earlier, the specifications for the transmitter based on the important transmitter parameters are as follows

Optical power output: - In an outdoor optical link, one of the most important transmitter parameter is the amount of optical power that the transmitter can emit in to air with respect to the dc drive current supplied. From the optical power budgeting considerations [1, 13], we found out the minimum average optical power required at the transmitter end at 40 Mbps to be

$$P_T = P_R + C_L + M_a \text{ dBm} \quad \ldots\ldots(3.11)$$

where,

P_T --- minimum average power required at the transmitter to give full modulation depth at 40 Mbps,

P_R --- minimum average power required at the receiver at 40 Mbps,

C_L --- total losses in dBm,

M_a --- safety margin.

The receiver sensitivity was specified as –28.9 dBm. The total channel loss applied to a free space environment for a point-to-point link that operates with a slightly diverging beam would be 20 dB [15]. C_L includes atmospheric attenuation, scintillation, mis-pointing errors, receiver optical loss and geometrical spreading losses. The safety margin M_a depends to a large extent on the system components as well as the system design procedures and is typically in the range of 5-10 dB. Systems using injection laser transmitter generally require a larger safety margin (e.g. 8 dB) than those using a LED source (e.g. 6 dB) because the temperature variation and ageing of the LED are less pronounced. So we have the minimum required optical power output of the transmitter,

$$P_T = -28.9 + 20 + 10$$

$$= 1.1 \text{ dBm (1.28mW) of optical power.}$$

Eye safety: - The maximum optical power out put of the transmitter is limited by the eye safety considerations as given in Table 2.1. Out door point to point systems generally use high power lasers that operate in the class 3B band (2.5-500 mW) to achieve a good power budget. Hence the optical power out put of the transmitter source can be from 1.28-500 mW for wavelength of 0.8-0.9 nm ranges. The safety standards recommend that these systems should be located where the beam cannot be interrupted or viewed inadvertently by a person. Roof top locations or high walls are usual for this type of systems.

Speed of response: - The response of an optical source to a current step input is often specified in terms of the 10-90 % rise time, a parameter which is reciprocally related to the device frequency response. The rise time of many available LEDs lie between 2 and 50 ns and give 3 dB bandwidth of around 7 to at least 175 MHz. Stimulated emission from injection lasers occur over a much shorter period giving rise times of the order of 0.1-1 ns, thus allowing 3 dB bandwidth above 1 GHz. However injection laser performance is limited by the device switch on delay, hence to achieve highest speeds it is therefore necessary to minimize the switch on delay. But as per our system specifications, the transmission bandwidth is only 30 MHz and hence is not that critical.

The total rise time degradation of a link should not exceed 70% of a NRZ bit period or 35% of a RZ bit period, where one bit period =1/ data rate. Also as per rise time budget, [1]

$$t_{sys} = 1.1\left[t_s^2 + t_d^2\right]^{1/2} \quad \text{.....(3.12)}$$

where,

t_{sys} =__ total rise time of the link in ns,

t_s =- rise time of the transmitter source in ns

t_d = rise time of the detector in ns

From this, the transmitter source rise time was calculated as $t_{tx} < 15$ns, for a NRZ with 40 Mbps data rate, assuming t_d as 5 ns which is a typical value for p-i-n diodes.

Beam divergence : - Transmit beam spreads constantly with increasing range at a rate determined by the divergence as shown in Fig. 3.7. . This gives rise to geometrical

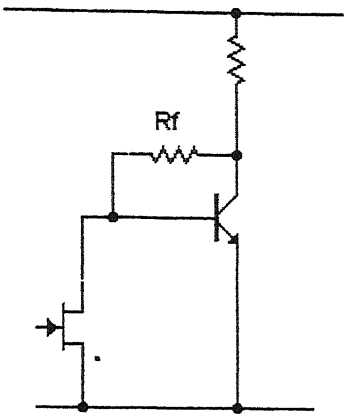

Fig. 3.6. Common source FET with shunt feedback stage.

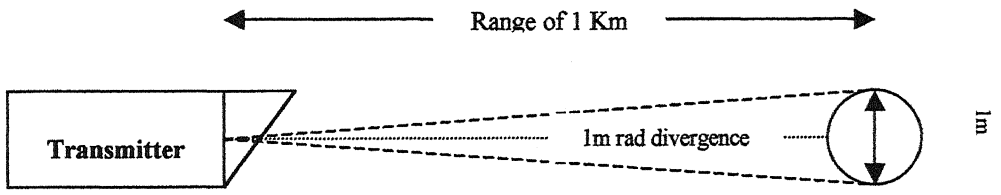

Fig. 3.7. Beam divergence.

spreading [13].

$$\text{Geometrical spreading loss} = 10 \log \left[\frac{\text{Surface area of receive aperture}}{\text{surface area of transmit beam at range } R} \right] dB \quad (3.13)$$

$$= 10 \log \left[\frac{SA_R}{SA_T + \frac{\pi}{4}(\theta R)^2} \right] dB$$

where,

SA_R = Surface area of receive aperture,

SA_T = Surface area of the transmit aperture divergence,

θ = Angle in radiance,

R = Range in metres.

As the range specified in our link was >40 m, the geometrical spreading loss was kept as <10 dB, as the total channel loss specified was only 20 dB.

Thermal behaviour: - The thermal behaviour of optical source can limit their operation with in the optical transmitter. Threshold currents of AlGaAs devices for example, increases by approximately by 1% per degree centigrade increase in junction temperature. Hence any significant increase in junction temperature of the injection laser may cause loss of biasing and a subsequent dramatic reduction in the optical output power. Hence an optical feedback circuitry is required to be incorporated to maintain a constant optical output level from the device.

Extinction ratio penalty : - It is defined as the ratio of the optical energy emitted in the '0' bit period to that emitted during the '1' bit period. For an ideal system it should be zero. But since injection lasers are prebiased during a '0' bit period, some optical power will be emitted during the pulse. Typical extinction ratios are 0.05-0.1 and such non-zero values give rise to noise penalty, called extinction ratio penalty within the optical link. In practice it is found to be in the range of 1-2 dB.

Cost : - The cost of the transmitter should be as low as possible and should use readily available components. The circuit should be simple and easy to design and fabricate.

The summary of specification for the transmitter is given in Table 3.2.

Sl No	SPECIFICATION PARAMETER	VALUE
1	Optical power	1.28-500 mW
2	Eye safety	Class 3B or lower
3	Speed of response	Rise time <15 ns
4	Geometrical spreading loss due to beam divergence	<10 dB
5	Extinction ratio penalty	<2 dB
6	Complexity of circuit	Simple
7	Cost	Moderate
8	Reliability	High
9	Time	<2 month

Table 3.2. Summary of specifications for transmitter

3.2.2 CHOICE OF OPTICAL SOURCE

The optical source is often considered to be the active component in the optical communication system. The fundamental function is to convert electrical energy to optical energy in an efficient manner. The major requirements are: -

a) The light output should be highly directional.

b) Must accurately track the electrical input signal to minimize distortion and noise. Ideally, the source should be linear.

c) Should emit light at wavelengths where the detectors are efficient and atmospheric losses are low.

d) Capable of simple signal modulation (i.e. direct) over a wide bandwidth extending from audio frequencies to beyond the gigahertz range.

e) Must be capable of maintaining a stable optical output which is largely unaffected by changes in ambient conditions (e.g. temperature)

f) It is essential that the source is comparatively cheap and highly reliable in order to compete with conventional transmission techniques.

The semiconductor lasers because of its compact size and capability for high frequency modulation is one of the most important light sources. Though they are similar to other lasers such as solid-state ruby lasers and He-Ne gas lasers, they differ in the following respects:

a) In conventional lasers, the quantum transition occur between discrete energy levels, whereas in semiconductor lasers the transitions are associated with band properties of materials.

b) A semiconductor laser is very compact in size (of the order of 0.1 mm long). In addition since the active region is very narrow (of the order of 1μm thick or less), the divergence of the laser beam is considerably larger than in conventional laser.

c) The spatial and spectral characteristics of a semiconductor laser are strongly influenced by the properties of the junction medium (such as band gap and refractive index variations).

d) For the p-n junction laser, the laser action is produced by simply passing a forward current through the diode itself. The result is a very efficient overall system that can be modulated easily by modulating the current. Since semiconductor lasers have very short photon life times, modulation at high frequencies can be achieved.

There are a multitude of semiconductor laser types usable as transmitter sources for outdoor optical wireless links. Particular laser types are generally identified by the type of material that is used as the 'gain medium'. Selection of which laser family to be used for a particular communication system is dependent upon a number of factors including link range, propagation medium and data rate. Fig. 3.8 shows the range of laser emission wavelengths for various semiconductors from near ultraviolet to far infrared [6].

All lasers, no matter what type operate on the same principles. A laser consists of an extremely high Q-cavity resonator built around an energy amplifier (Fig. 3.9. [4]). Exciting or pumping the medium to a higher-level metastable energy state achieves amplification. Lasing will commence (threshold) when optical gain just equals roundtrip optical loss.

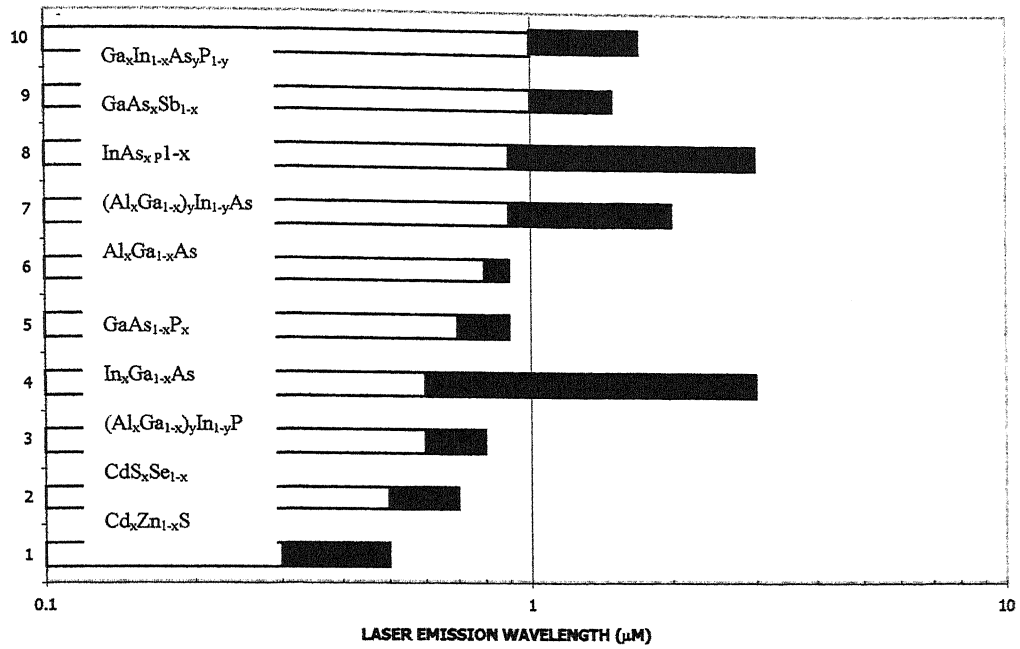

Fig. 3.8. Emission wavelengths potentially available for various hetrostructure lasers at 300K

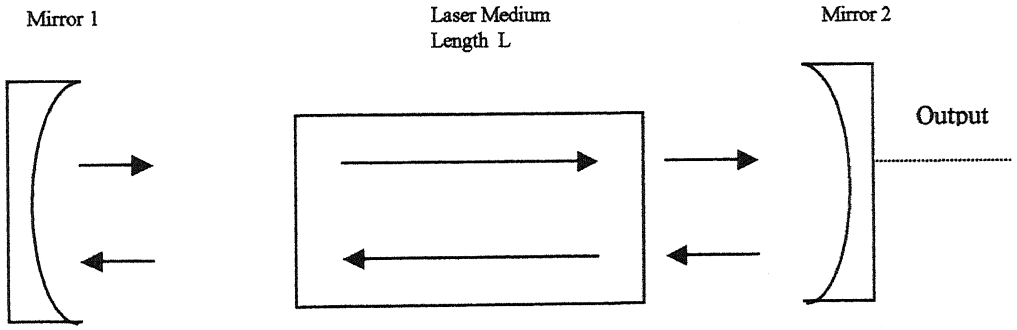

Fig. 3.9. Fundamental elements of a laser

3.2.3 TRANSMITTER DESIGN

For our study a simple laser transmitter was designed using commercially available low cost key-chain laser as source. The transmitter circuit basically consists of a pre-biasing circuit and a driver circuit as shown in Fig. 3.10. The circuit does not have any feedback circuit for maintaining constant bias current in order to maintain a constant optical output power. Another consideration not addressed is the laser protection circuit. Laser diodes are easily damaged by spurious electrical spikes or surges. Commercial laser transmitter circuits provide elaborate protection circuits to guard against these spurious spikes. The laser transmitter circuit must be handled very carefully. A 47 K ohms potentiometer was included in series with the laser to avoid switch-on and switch-off surges, which may damage the laser. (In the course of fabrication of the transmitter, about 3 lasers got damaged).

Pre-biasing circuit is designed such that it allows a dc current of value just below the threshold current of the laser to flow when the data input is a '0'. Driver circuit is designed such that it allows a dc current of maximum permissible value to flow through the laser, when the data input is a '1'. Details of the circuit will be given in Chapter 4.

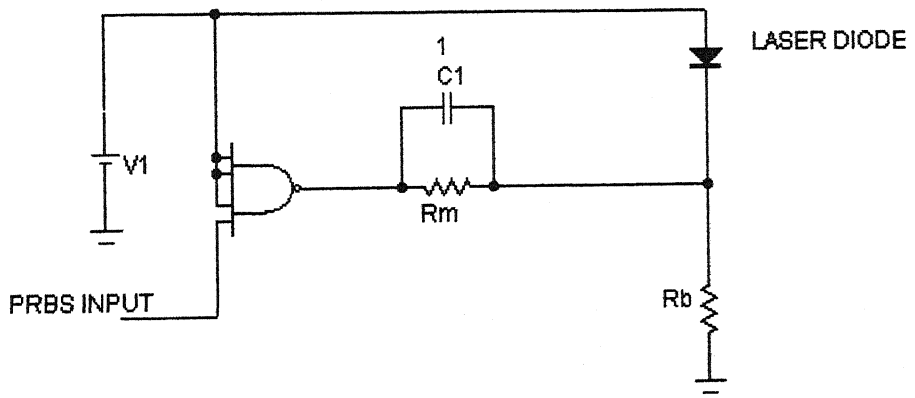

Fig. 3.10. Transmitter circuit.

CHAPTER 4

IMPLEMENTATION OF AN OUTDOOR HIGH SPEED OPTICAL WIRELESS LINK

A high-speed outdoor wireless optical link was successfully implemented using discrete components available in the laboratory within the given time of six months. In this chapter the implementation of the receiver circuit, transmitter circuit as well as the establishment of an out door optical wireless link using these is discussed in detail. Also, design verification using SPICE circuit simulator is included in this chapter.

4.1 RECEIVER CIRCUIT

A PIN diode with JFET as the front end amplifying device and a shunt feedback stage with BJT formed the preamplifier stage of the receiver. The photodetector used was C30808, N-type silicon p-i-n photodetector of RCA, whose data sheet is attached in Appendix A. The JFET used was BFW10, N-channel silicon field effect transistor of BEL. The data sheet of BFW10 is attached as Appendix B. The BJTs used were from the high frequency N-P-N transistor array CA3127E of RCA, whose data sheet is also attached as Appendix C. The preamplifier stage of the receiver circuit is shown in Fig. 4.1 (a).

The second stage of the receiver consists of the post amplifier, comparator and the line driver. The preamplifier output of about 160 mV at –28.2 dBm was amplified further using the LM733C video amplifier, whose data sheet is attached as Appendix D. Out of the three gain settings of LM733C, viz. 10, 100 and 400, the maximum gain of 400 was chosen. The post amplifier output was fed to the NE529 high-speed comparator to obtain a TTL compatible signal. Data sheet of NE529 is attached as Appendix E. The reference

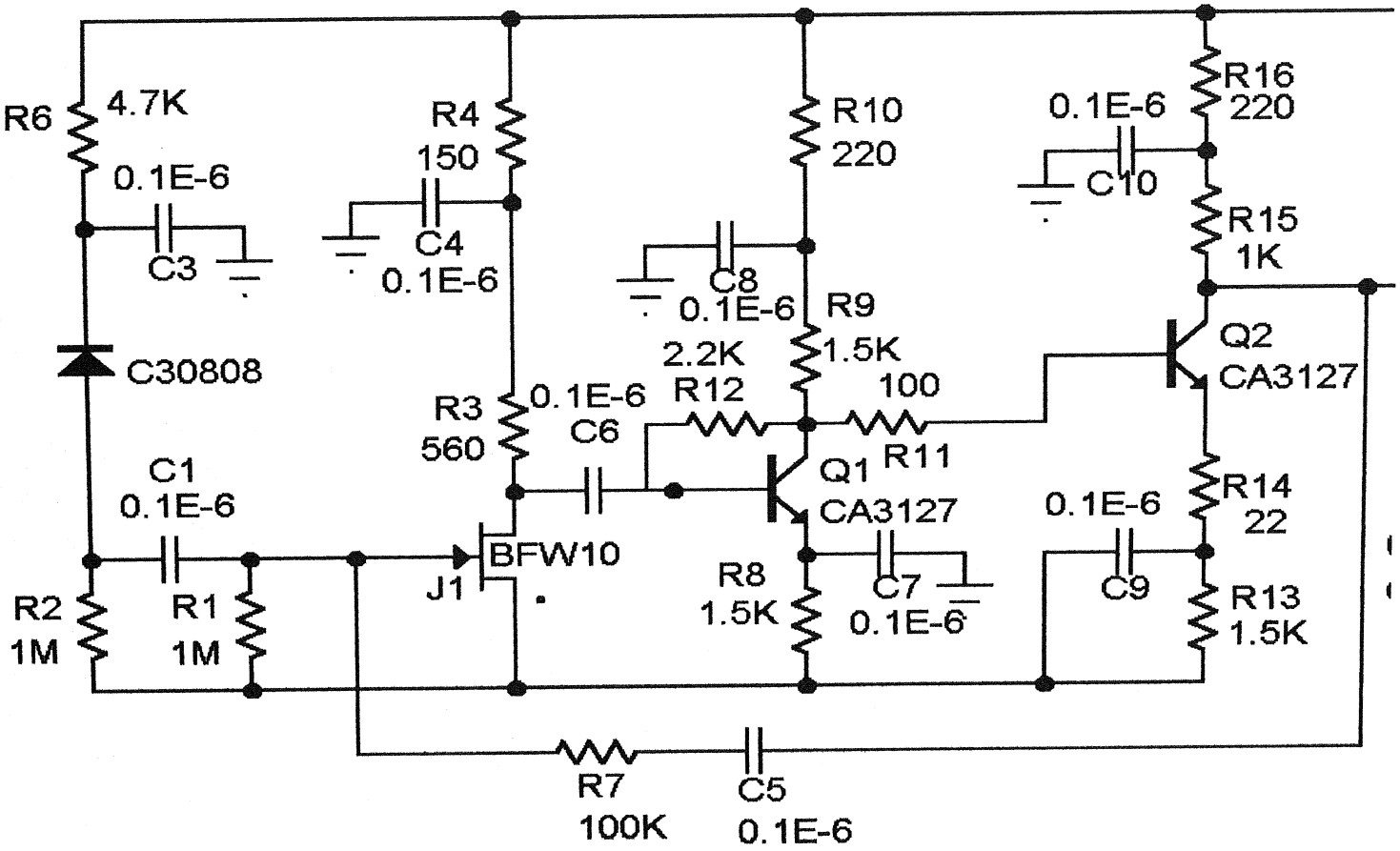

Fig .4.1. (a) Preamplifier circuit.

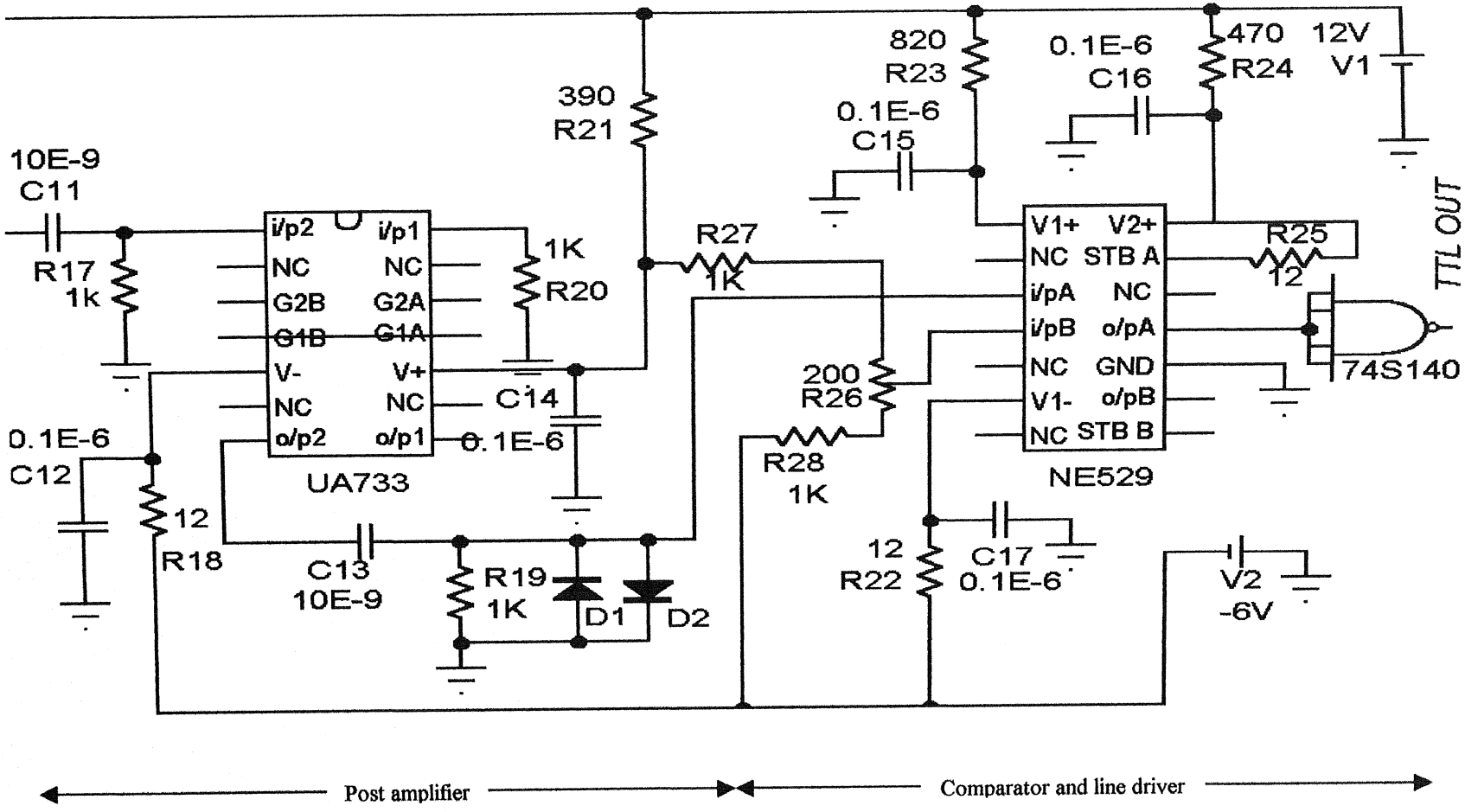

Fig. 4.1. (b) Second stage of receiver circuit

input was fine tuned using a resistor network. Finally, this signal was fed to a 74S140 line driver for facilitating 50 ohm driving capability. The second stage of the receiver circuit is shown in Fig. 4.1 (b).

4.2 SPICE MODELLING, SIMULATION AND ANALYSIS

Before wiring up on a breadboard, the preamplifier circuit was simulated on a circuit simulator package for verification of design. The software used was Micro-cap evaluation demo version 6.1.9.0.

Equivalent circuit used to represent the detector was a current source shunted by the depletion capacitance, C_d of the detector [2]. Series resistance and shunt conductance should have also been added to the equivalent circuit, but since both are small, having negligible effect on performance, were omitted from the equivalent circuit for convenience.

Dark current flowing in the detector in laboratory conditions was measured using the circuit shown in Fig. 4.2. It was found to be 6.3nA, whereas as per the data sheet it should have been within 5 nA. This is due to the ambient light that has to be accounted for. This measured value of dark current was used as the dc value of the current source. The magnitude of peak current flowing through the detector when light falls on it, assuming worst conditions (i.e. max data rate and the minimum specified received power for detection at a BER of 10^{-9}) was calculated as follows:

Responsivity of detector = 0.6 A/W as per data sheet,

Sensitivity of Receiver as specified = -28.9 dBm at 40 Mbps,

Peak power = -28.9 + 3 dBm, (= 2.57 μW)

$\therefore$ Peak current, I_p = $0.6 \times 2.57 \times 10^{-6} = 1.542$ μA.

. Thus for circuit simulation, the computational model of the photodetector as shown in Fig. 4.3 (a) and (b) were used for AC analysis and Transient analysis response. In AC analysis, the current source was represented as an AC source with DC value equal to 6.3 nA(dark current) and the magnitude of AC equal to 1.542 μA (I_p). For transient analysis, the current source was a PULSE source with i_1 =6.3 nA, i_2 = 1.542 μA, t_d = 0, t_r = 1E-9, t_f = 1E-9, pw = 25E-9, per = 50E-9, assuming a 1010... data pattern with $t_r = t_f$

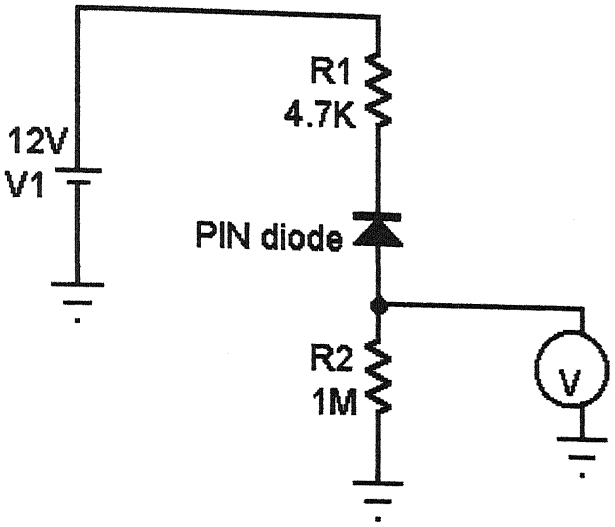

Fig. 4.2. Set up for measuring the dark current under lab conditions.

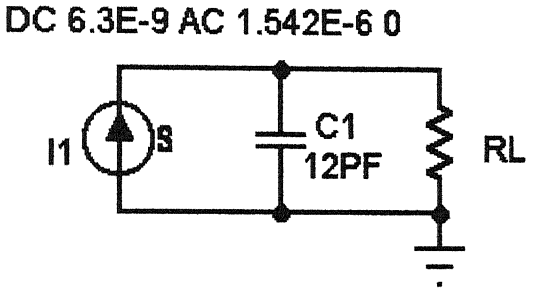

(a) AC analysis model

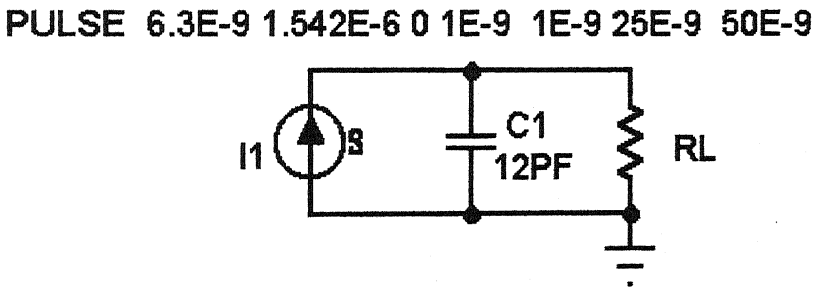

(b) Transient analysis model

Fig. 4.3. Computational model of photodetector used for circuit simulation

PARAMETERS	EXTRACTED VALUE[24]
BETA	8E-4
LAMBDA	6.7E-3
VTO	-3.53
CGD	10PF
CGS	4.5PF

Table 4.1 Important model parameters and values of JFET BFW 10

PARAMETERS	EXTRACTED VALUE[24]
BF	96
IS	1.33E-16
BR	1
VAF	20
RB	15
RE	4
RC	21
CJE	0.6PF
CJC	0.4PF
CJS	2.175PF
MJS	0.33
TF	134PS
TR	1.34NS

Table 4.2 Important model parameters and values of CA3127

=1 ns for the laser source.

Important model parameters used for the JFET (BFW10 N-channel silicon FET) and the BJT (CA3127E) in circuit simulation along with their extracted values are given in Table 4.1 and 4.2.These parameters were extracted in an earlier work [24].

The ***AC analysis*** of the circuit was done to evaluate the frequency response of the preamplifier circuit. The circuit used for simulation is shown in Fig. 4.4 along with the node numbers and the dc currents highlighted. The plots of output voltage vs frequency, gain vs frequency and phase vs frequency are shown in Fig. 4.5. The 3 dB bandwidth was found to be 19.9 MHz with a flat response up to a frequency of 10 MHz. The preamplifier output voltage was 152.21 mV.

By adding a small capacitance value across the feedback resistance and varying it the effect of parasitic capacitance was simulated [23]. Even in the pF range it was observed that as capacitance increases, bandwidth decreases drastically. The plot is shown in Fig. 4.6. The importance of keeping the parasitic capacitance to a minimum while fabricating the PCB was driven home.

Plot for different values of feedback resistance, R_f from 1K to 900K ohms in steps of 100K ohms is shown in Fig. 4.7. The relation between R_f and bandwidth was better understood by this simulation. Optimum value of R_f for a 2 V p-p out put was found to be 100 K, whose corresponding value of 3dB bandwidth was 19.95 MHz.

The ***transient analysis*** was done to evaluate the response of the circuit to a 40 Mbps NRZ pulse at the specified sensitivity of –28.9 dBm. The simulation plot is shown in Fig. 4.8 (a). The simulation was repeated for a 20 Mbps pulse. The plot is shown in Fig. 4.8 (b). From this we can infer that beyond 40 Mbps the performance of the circuit will deteriorate drastically due to the capacitive effect of the photodetector and the BER will increase rapidly.

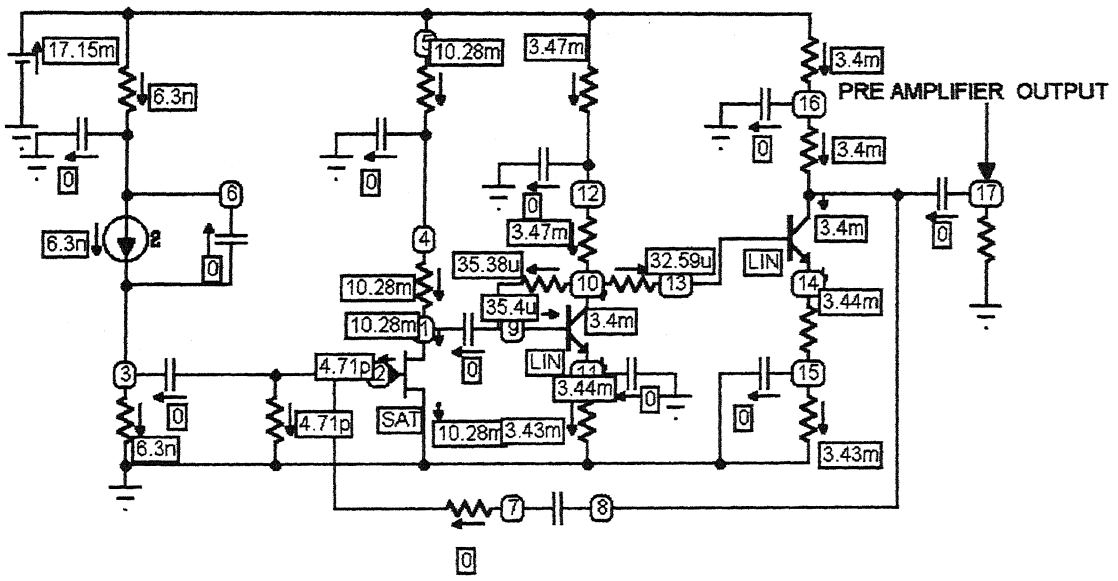

Fig. 4.4. Preamplifier circuit used for AC analysis showing the node numbers and the dc currents

4.3 THE TRANSMITTER CIRCUIT

The transmitter circuit was implemented using a laser source from a key chain laser available in shops for about Rs. 70/-. This was not only cheap but also readily available. The laser was taken out from the metal casing by carefully cutting open the casing with an axon blade and bypassing the switch by soldering two wires directly onto the terminals of the laser. The circuit is shown in Fig. 4.9 in detail.

In order to set the biasing and modulating currents as discussed in the previous chapter we have to know the threshold current of the of the laser being used. For this purpose optical power output of the laser (L-I characteristics) was measured and is plotted in Fig. 4.10. While doing this experiment care was taken to ensure that there is no loose connection anywhere in the circuit as there is a danger of the laser getting damaged due to the transients.

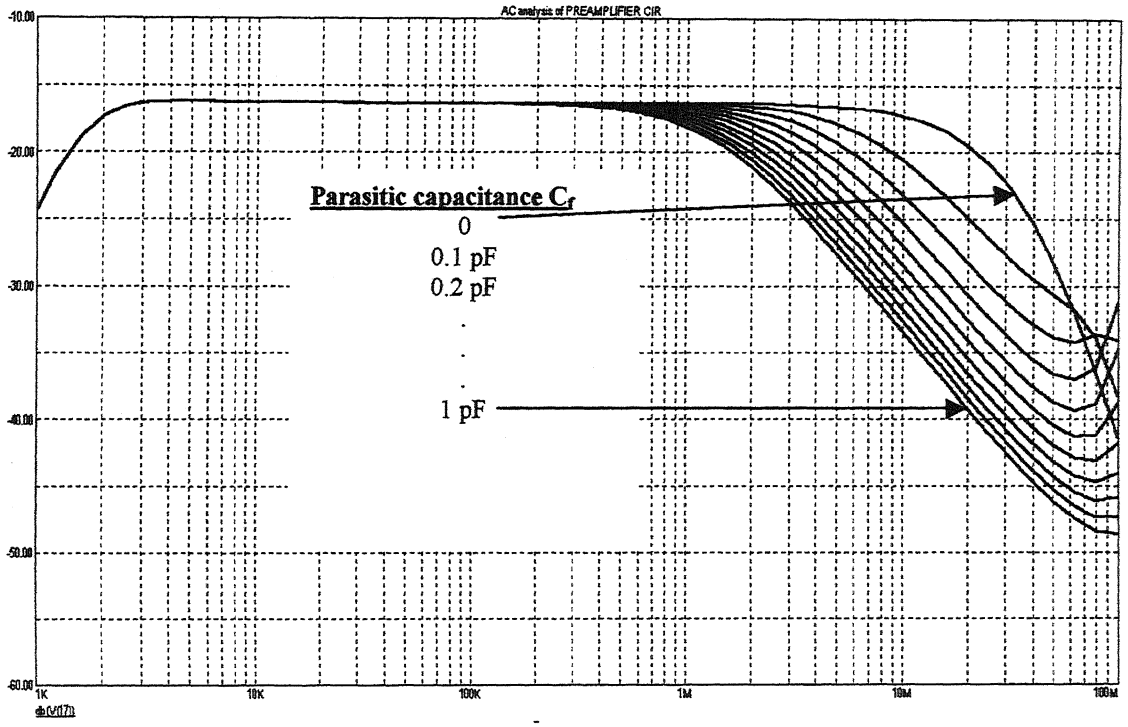

Fig. 4.6. Gain vs Frequency plot for different values of C_f

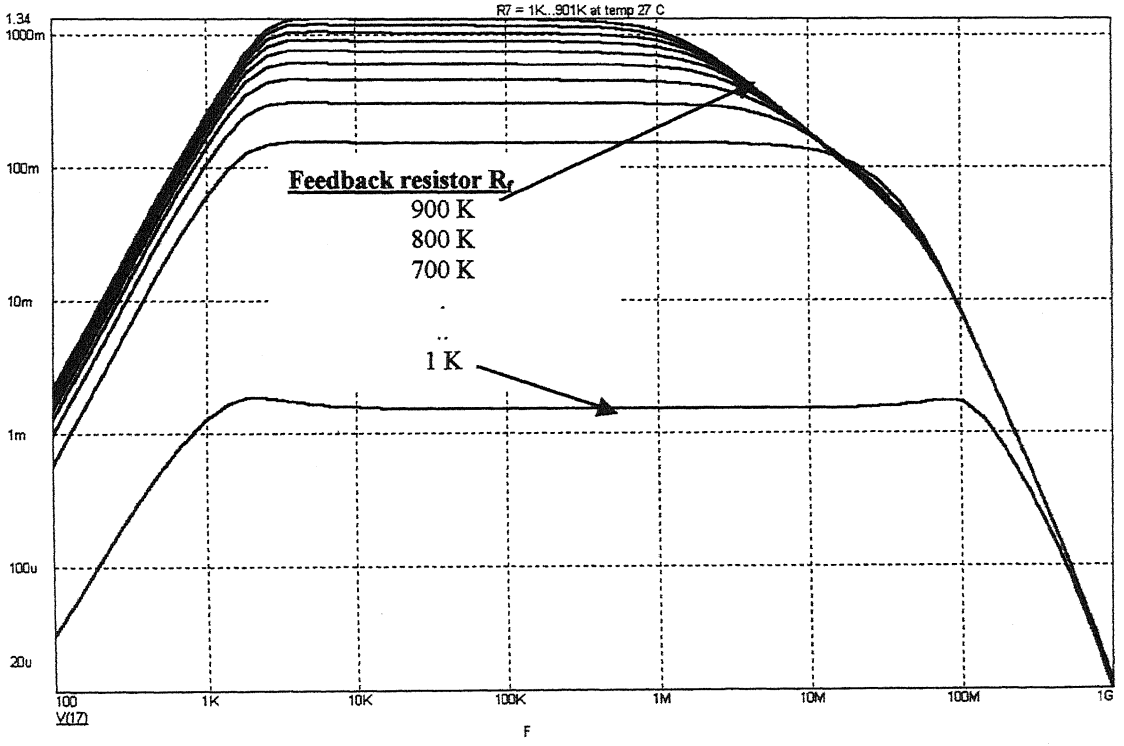

Fig. 4.7. Output voltage vs Frequency plot for different values of R_f

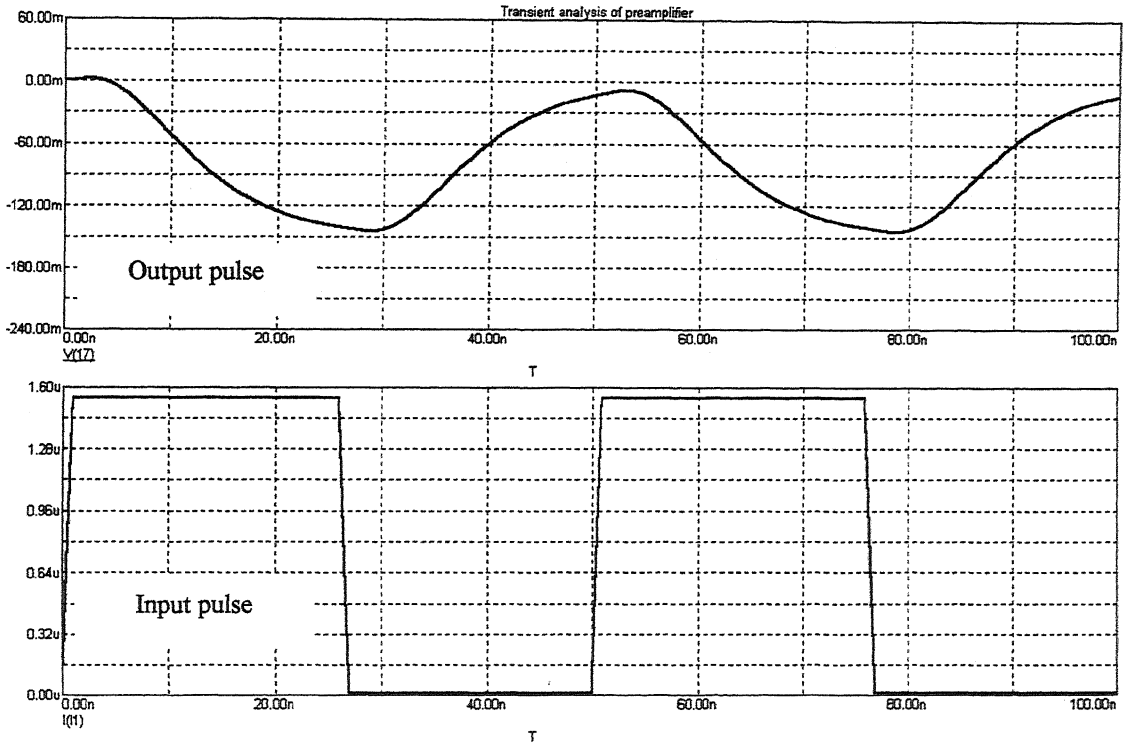

(a) at 40 Mbps

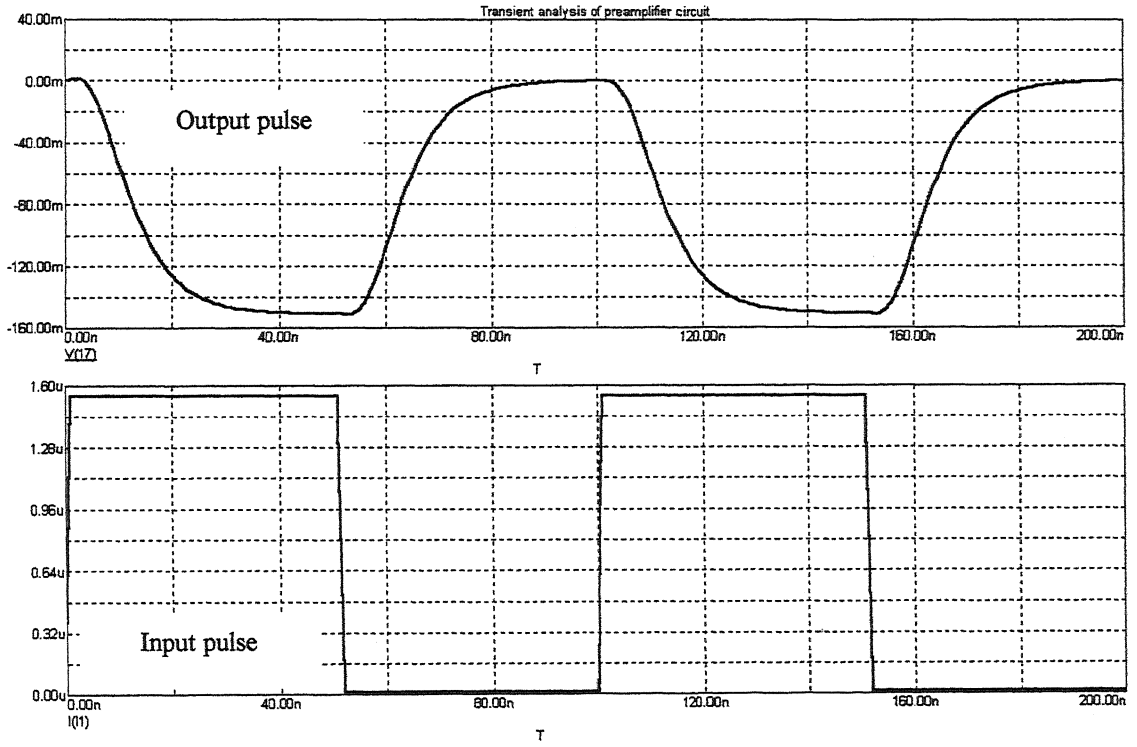

(b) at 20 Mbps

Fig. 4.8. Transient response of the preamplifier circuit at sensitivity of –28.9dBm.

4.4 FABRICATION ON A PRINTED CIRCUIT BOARD

The transmitter and the receiver circuit designed were fabricated on a printed circuit board (PCB). But before that, the circuit was wired up on a breadboard and the values checked with the simulated results.

The main problems, which can come up in a PCB design, are reflections, cross talk, ground and supply line noise and EMI from pulse type EM field [25]. Hence the following high frequency design rules were kept in mind while preparing the layout of the PCB.

- Length and width of signal conductor should be as small as possible.
- The signal and ground conductors should not be too close as this capacitance along with the output resistance acts as LPF.
- Proximity of input and output conductors should be avoided as this will lead to Miller effect.
- Cross talk can occur if two signal lines run parallel to each other for a length more than 10 cm.
- Measures to reduce ground and supply line noise are to have low impedance between the supply line and the ground line by having broad conductors close to each other. Also by providing an electro magnetically stable ground by having large copper surface for ground , we can reduce the noise.
- Mains filtering and providing separate shielding for it reduces the EMI from pulse type EM fields.

The whole assembly was shielded using a mild steel box, which enhanced the performance of the receiver by at least 2 dB, and also the output was much more stable.

4.5 EXPERIMENTAL SETUP

The high-speed optical wireless link was set up as shown in Fig. 4.11. Alignment of the laser beam was done visually by observing it on a white background and then bringing the detector slit on the receiver to the centre of the beam. Mounts with the capability of precise movements in two axes were used for mounting the receiver and transmitter. The receiver and transmitter were set up at 5m apart and it was found that the

receiver was getting saturated. The received power was measured using a power meter and was–18.4 dBm When it was set up at 15m apart the received power was found to be –26.8 dBm and the receiver was detecting perfectly up to 13 Mbps. From 13 Mbps onwards, the timing errors started appearing, though all the bits were being received. At 16.8 Mbps the receiver performance deteriorated. The plot of the measured value of preamplifier output vs frequency is shown in Fig. 4.12.

To increase the bandwidth further the transistors used in the receiver were replaced with CA3227E (f_T >3MHz) instead of CA3127E (f_T >1 MHz). This gave a bit rate up to 20 Mbps without any deterioration, though from 14 Mbps onwards, timing errors started affecting the output.

For testing the link a 15 bit PRBS generator was used. The circuit of PRBS generator used is shown in Fig. 4.13. The PRBS sequence generated was 110010001111010. An auto start circuit was also incorporated in the PRBS generator with 4-input NOR gates (7425) to prevent the circuit from locking in the event of '0000' state at start.

While testing the link outdoors it was found that the ambient light was very high (almost –8dBm). Hence the receiver had to be placed in such a way to prevent direct sunlight falling on it. A simple red filter (red translucent cellophane sheet) was used in front of the photodetector to further enhance the performance. This reduced the ambient light by about 5 dB.

The CRO used was a 150 MHz COS 6150 oscilloscope of Kikusui Electronics Corporation. The other equipments used were a function generator, Model 4502 Kikusui Electronics Corporation and an optical power meter, Model LP 5000 of Nettwt.

Power supply requirement was met from compact, SMF (sealed, maintenance free) lead acid batteries of 6v and 12v, which reduced the supply noise considerably.

In order to prevent damage of the laser transmitter the following precautions were taken. Since lasers are highly sensitive to static and other surges, all forms of transient should be prevented from reaching laser. This was ensured right from cutting open the key chain laser cover to the stage when the laser is soldered on to the circuitry. A diode was connected across the laser to bypass reverse bias transients. A 75 Ω resistor, which

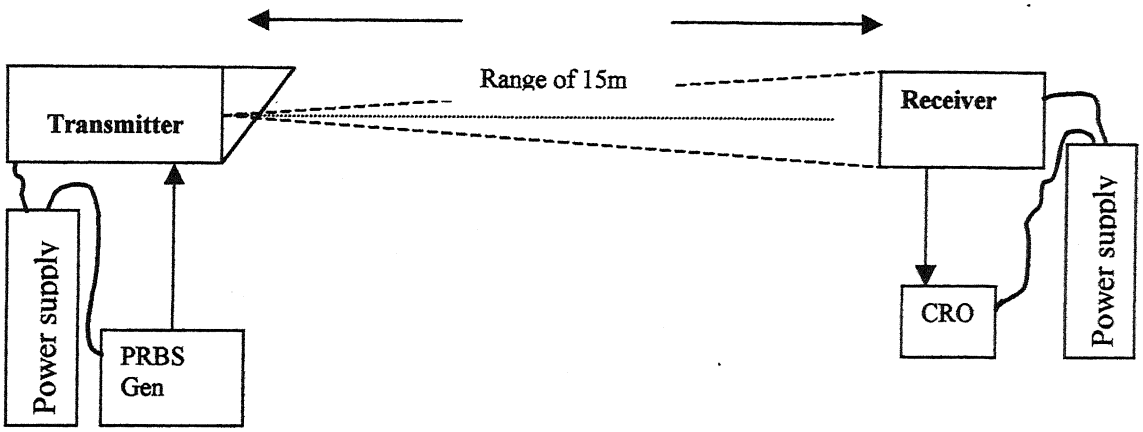

Fig 4.11 Experimental set up

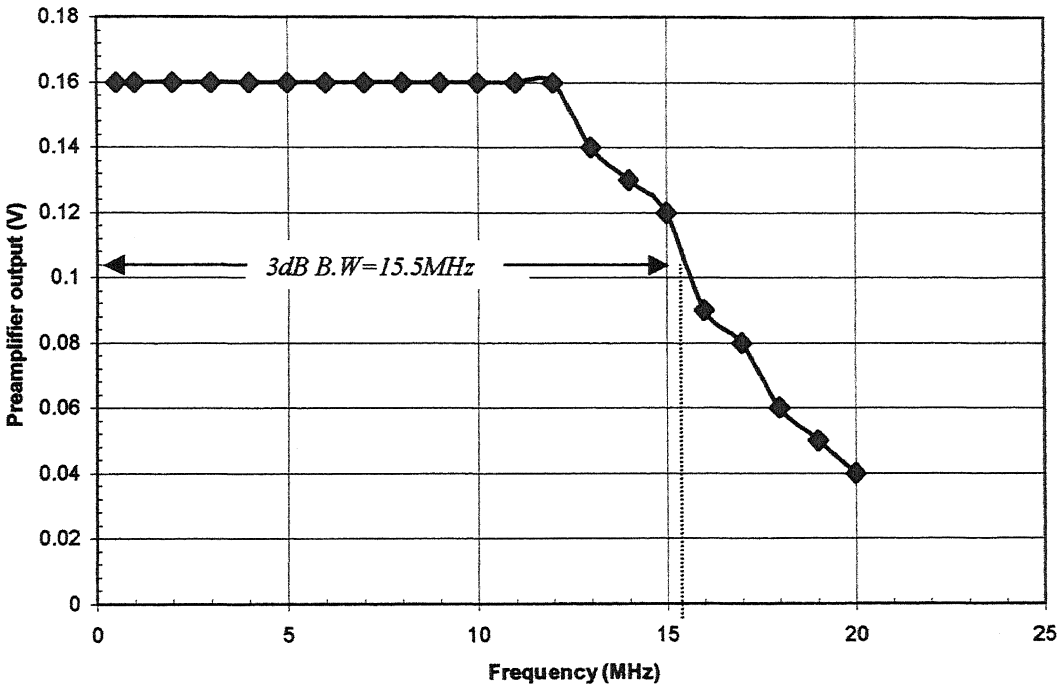

Fig 4.12. Experimentally obtained frequency response plot.

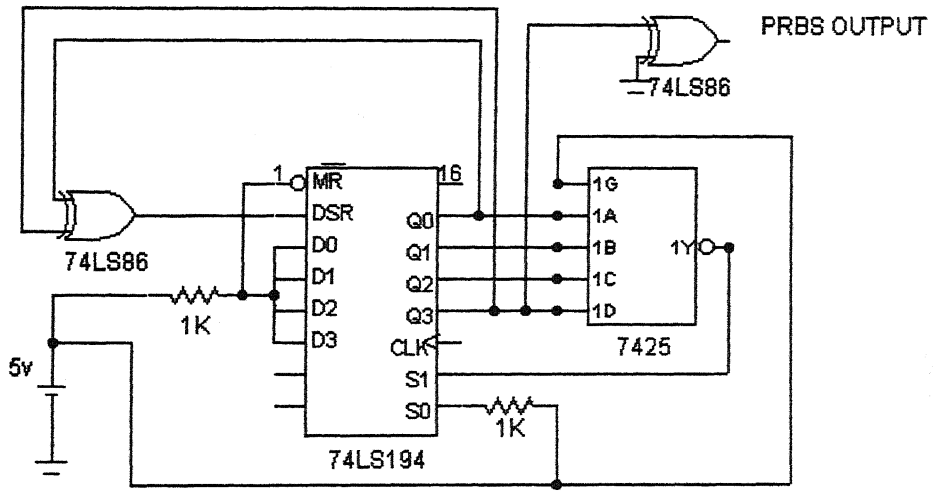

Fig 4.13 PRBS generator

already existed in the PCB of the key chain laser, was allowed to be in series with the laser. This gave protection against over biasing. The switching-on/off procedures given below were strictly followed:

a) All cable connections were given before switching –on the power supply.

b) Ensure that 47 K ohms potentiometer is in the maximum resistance position before switching-on.

c) Turn-on the power supply and slowly bring the voltage up to 5V.

d) Slowly vary the 47 K pot from maximum resistance position to minimum resistance position keeping an eye on the laser output.

e) Check the power output of the laser with a power meter.

f) While switching-off, first increase the 47 K pot position from minimum resistance position to maximum resistance position.

g) Slowly reduce the power supply voltage to zero voltage.

h) Switch-off the power supply after waiting for two minutes.

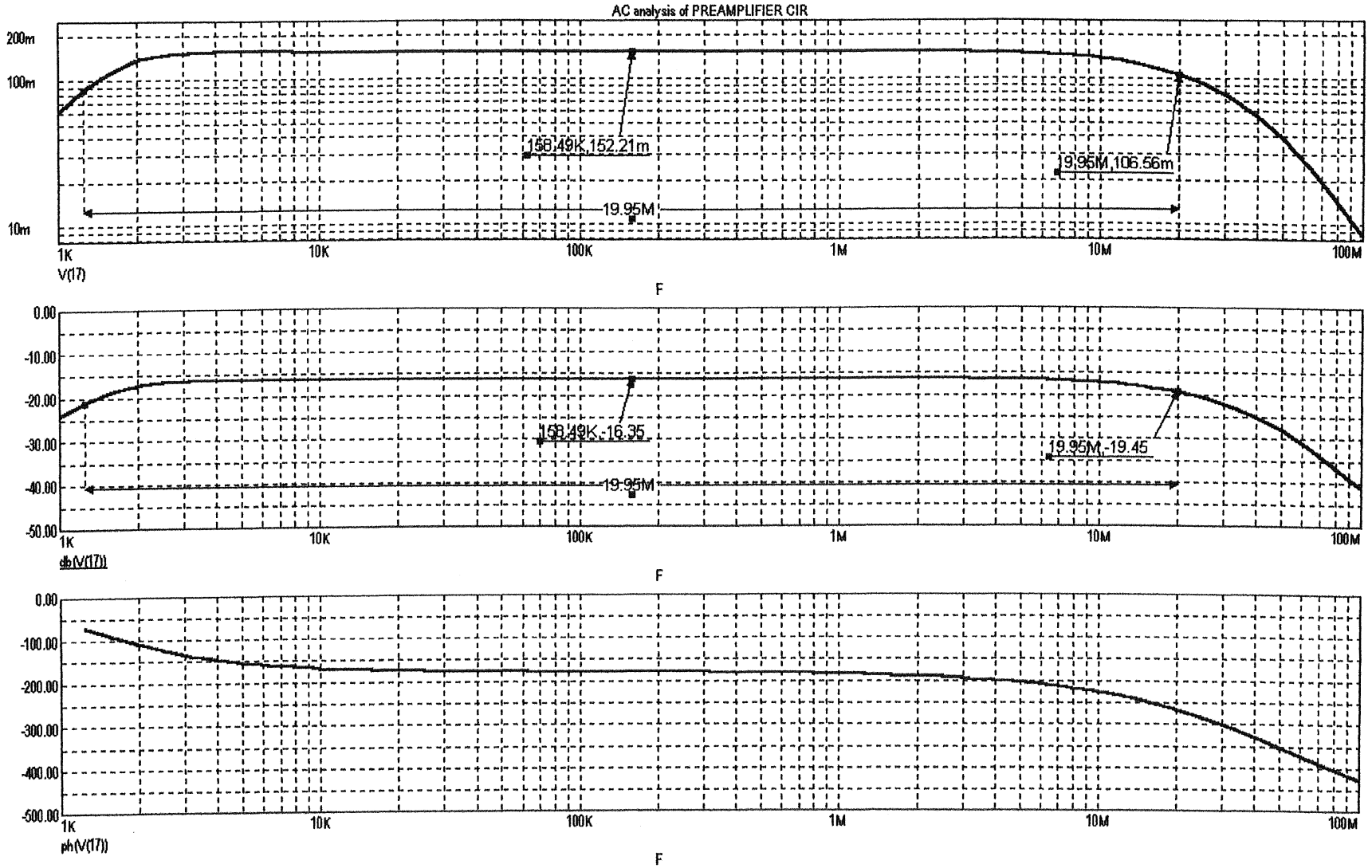

Fig. 4.5. AC analysis of preamplifier circuit showing the output voltage, gain (dB) and phase plots.

CHAPTER 5

SUMMARY AND CONCLUSION

A 20 Mbps outdoor wireless optical link has been successfully implemented using discrete components available in laboratory, which is capable of communicating at a distance of 20 m apart under clear weather.

The laser transmitter gave an average power output of –7 dBm at the transmitter end. The receiver sensitivity was –28.2 dBm at 20 Mbps. The losses were approximately 21 dB, mainly due to the geometrical spreading of the beam. Hence the link margin was 0.2 dB, which is in fact very less for a reliable operation of the link.

The geometrical spreading loss was much more than estimated since we used a cheap laser source whose beam divergence was large. Also the power output of the laser beam was less than what was specified. Hence the distance specified could not be achieved for the link. Use of a better source or concentrators at the receive end to concentrate the beam on to the detector, can help in achieving the target of 40 m. The summary of specifications given for the high-speed optical link and the actual value obtained practically are shown in Table 5.1. Thus it can be concluded that wireless optical communication is an attractive, reliable and cost effective method of linking up the high speed data available through the fiber optical links already in place, to the terminal equipments of the user, thus solving the problem of the last mile bottle neck.

RECOMMENDATIONS FOR FURTHER WORK

Technological improvements that can be done to the present system are: -

a) Use of filters to reduce ambient light at the receiver end.

b) Use of concentrators at the receiver end to nullify the effect of beam divergence

Sl No	PARAMETER	TARGET SPECIFIED	TARGET ACHIEVED
1	Bit rate	>40 Mbps	20 Mbps
2	Distance	>40 m	20 m
3	BER	$<10^{-9}$	$<10^{-9}$
4	Receiver sensitivity	Better than -28.9 dBm	-28.2 dBm
5	Dynamic range	>15 dB	<10 dB
6	Cost	Moderate	Low cost (used only discrete components available in the lab)
7	Reliability	High	Medium
8	Circuit complexity	Simple	Simple
9	Time for development	< 6 months	6 months

Table 5.1 Summary of target specified and achieved.

and thus reduce geometrical spreading loss.

c) Better transmitter circuitry for optical feedback control to maintain a constant power output.

d) Possibility of increasing the power output of the transmitter by power combining of the transmitter sources.

e) Instead of a fixed threshold comparator used in the receiver circuit use of a peak detector and summing amplifier circuit can improve the timing errors considerably.

f) Though AC coupling improves sensitivity over DC coupling for a large temperature range, AC coupling confines the input signal to a constant average value for all, time intervals. NRZ coding with a long string of '1's and '0's cannot be, for example, be reproduced across the coupling capacitor. An encoding scheme (Manchester coding), which has transition time in every bit time to keep the average value of the signal constant, must be used for such data.

REFERENCES

1 John. M. Senior, *Optical Fiber Communications*, 2nd ed.. New Delhi: Prentice-Hall of India, 1994.

2 R. G. Smith and S. D. Personick, "Receiver design for optical fiber communication systems", in *Semiconductor Devices for Optical Communication.* New York: Springer-Verlag, 1980.

3 Chinlon Lin (Ed), *Optoelectronic Technology and Lightwave Communication Systems.* New York: Van Nostrand Reinhold, 1989.

4 Morris Katzman (Ed), *Laser Satellite Communications.* Englewood Cliffs: Prentice Hall, 1987.

5 Pallab Bhattacharya, *Semiconductor Optoelectronic Devices.* New Delhi: Prentice-Hall of India, 1995.

6 S. M. Sze, *Physics of Semiconductor Devices*, 2nd ed.. India: John Wiley & sons, 1981.

7 T. V. Muoi, "Receiver design for high speed optical fiber systems", *Journal of light wave technology,* LT-2, pp 243-267, 1984.

8 K. Ogawa, "Considerations for optical receiver design", *IEEE Journal on selected areas in communications,* SAC-1, pp 524-532, 1983.

9 N. Shimizu et al., "40 Gbit/s monolithic digital OEIC composed of unitravelling-carrier photodiode and InP HEMTs", *Electronics Letters,* vol. 36, pp 1220-1221, 2000.

10 T. Takeuchi et al., "High speed, high power and high efficiency photodiodes with evanescently coupled graded-index waveguide", *Electronics Letters*, vol. 36, pp 972-973, 2000.

11 Y. Baeyens et al., "Millimetre-wave long wavelength integrated optical receivers grown on GaAs", *IEEE Photonics Technology Letters*, vol. 11, pp 868-870, 1999.

12 J. L. Gimlett, "Low-noise 8 GHz PIN/FET optical receiver", *Electronics letters*, vol. 23, pp 281-283, 1987.

13 I. I. Klm et al., "Wireless optical transmission of fast ethernet, FDDI, ATM, and ESCON protocol data using the TerraLink laser communication system", *Optical Engineering*, vol. 37, pp 3143-3155, 1998.

14 J. M. Kahn et al., "Wireless infra red communications", *Proceedings of the IEEE*, vol. 85, pp 265-298, 1997.

15 D. J. T. Heatley et al., "Optical wireless: The story so far", *IEEE Communication Magazine*, vol 36, pp 72-82, 1998.

16 M. Govindrajan, S. R. Forest, "Design considerations for wide band p-i-n /HBT monolithic transimpedance optical receivers", *Journal of Lightwave Technology*, vol. 11, pp 367-378, 1993.

17 M. Brian, T. P. Lee, "Optical receivers for light wave communication systems", *Journal of Lightwave Technology, vol.* 3, pp 1281-1300, 1985.

18 P. L. Eardley, D. R. Wisely, "1Gbit/s optical free space link operating over 40 m-system and application", *IEE Proc.-Optoelectron.*, vol.143, pp-330-333, 1996.

19 http://www.cablefree.co.uk

20 http://www.opticalaccess.com

21 http://www.it.uc.pt/oc

22 S. D. Personick, "Receiver design for optical fiber systems", *Proc. IEEE,* vol. 65, pp 1670 – 1678, 1977.

23 J. L. Hullett and T. V. Muoi, "A feedback receive amplifier for optical transmission systems", *IEEE Trans. Commun.*, vol. 24, pp 1180-1185, 1976.

24 M.Tandon and K. Agarwal, "Low noise receiver design for fiber optic communication links using PSPICE simulation", B.Tech Project Report, IIT, Kanpur, 1988.

25 W. C. Bosshart, *Printed Circuit Boards-Design and Technology.* New Delhi: Tata McGraw-Hill, 1983.

RCA Electronic Components

Solid State
Electro Optics
Developmental Types
C30807, C30808, C30809, C30810

N-Type Silicon p-i-n Photodetectors

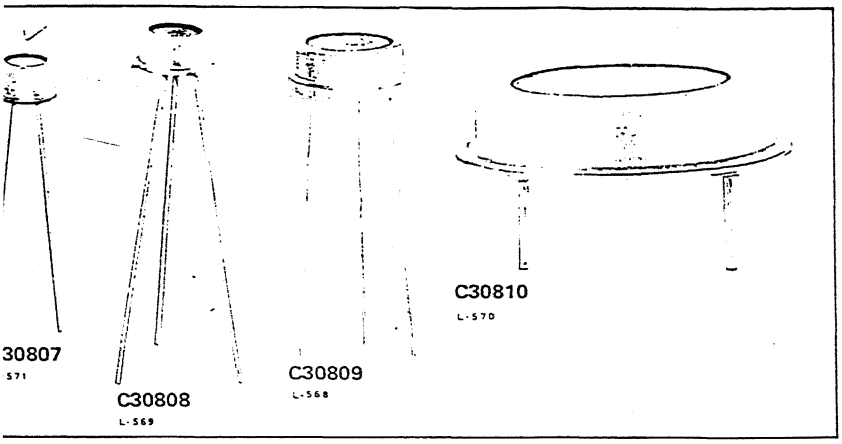

- Broad Range of Photosensitive Surface Areas — 0.8 mm^2 to 100 mm^2
- Low Operating Voltage — V_R = 45 V
- Anti-Reflection Coated to Enhance Responsivity at 900 nm
- Hermetically-Sealed Packages
- Spectral Response Range — (10% Points) 400 to 1100 nm

family of N-type silicon p-i-n photodiodes is designed se in a wide variety of broad band low light level appli- ns covering the spectral range from below 400 to over nanometers.

different types making up this series provide a broad e in photosensitive areas and in time response charac- ics. Each of the types is anti-reflection coated to en- e responsivity at 900 nanometers.

e characteristics make the devices highly useful in HeNe GaAs laser detection systems and in optical demodula- data transmission, ranging, and high-speed switching cations.

imum Ratings, Absolute-Maximum Values (All Types)

leverse Operating Voltage, V_R	100	max.	V
ɔcurrent, i_p:			
verage value, continuous operation	1.0	max.	mA
eak value	10	max.	mA
ard Current, I_F:			
verage value, continuous operation	10	max.	mA
eak value	100	max.	mA
ient Temperature:			
torage, T_{stg}	−60 to +100		°C
Operating, T_A	−40 to +80		°C

Mechanical Characteristics

	Type C30807	Type C30808	Type C30809	Type C30810
Photosensitive Surface:				
Shape	Circular	Circular	Circular	Circular
Area	0.8 mm^2	5.0 mm^2	50 mm^2	100 mm^2
Diameter	1.0 mm	2.52 mm	8.0 mm	11.4 mm

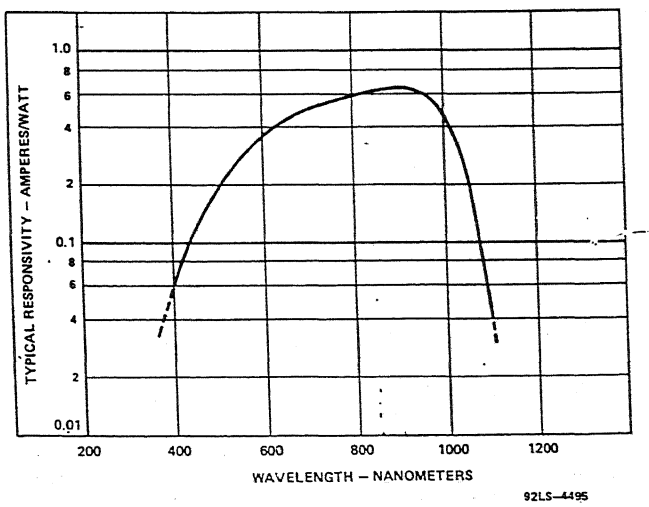

Figure 1 — Typical Spectral Responsivity Characteristic

urther information or application assistance on these devices, contact your RCA Sales Representative or write Solid State Electro Optics Marketing, RCA, Lancaster, PA 1760

opmental-type devices or materials are intended for

Information furnished by RCA is believed to be accurate and

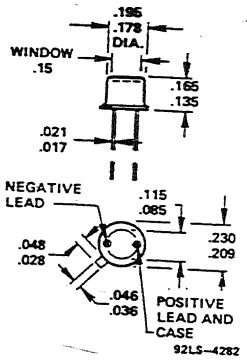

Modified TO-18

Figure 5 — Dimensional Outline for C30807

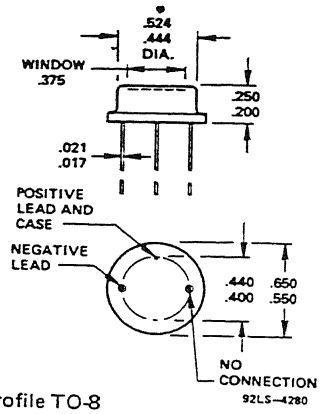

Low-Profile TO-8

Figure 7 — Dimensional Outline for C30809

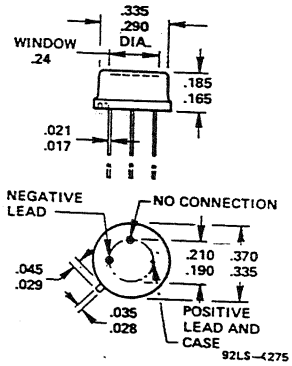

Low-Profile TO-5

Figure 6 — Dimensional Outline for C30808

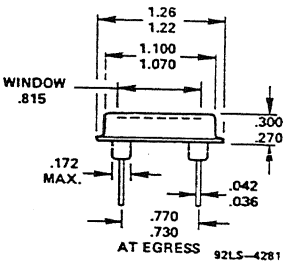

Custom

Note: Leads are labeled

Figure 8 — Dimensional Outline for C30810

N-CHANNEL SILICON FIELD EFFECT TRANSISTORS

N-channel silicon epitaxial planar junction field effect transistors in a TO-72 metal envelope with the shield lead connected to the case.
The transistors are designed for broad band amplifiers (0 to 300 MHz).
Their very low noise at low frequencies makes these devices very suitable for differential amplifiers, electro-medical and nuclear detector pre-amplifiers.

QUICK REFERENCE DATA

			BFW10	BFW11	
Drain-source voltage	$\pm V_{DS}$	max.	30		V
Gate-source voltage (open drain)	$-V_{GSO}$	max.	30		V
Total power dissipation up to $T_{amb} = 25\ ^{o}C$	P_{tot}	max.	300		mW
Drain current $V_{DS} = 15$ V; $V_{GS} = 0$	I_{DSS}	>	8	4	mA
		<	20	10	mA
Gate-source cut-off voltage $I_D = 0.5$ nA; $V_{DS} = 15$ V	$-V_{(P)GS}$	<	8	6	V
Feedback capacitance at f = 1 MHz $V_{DS} = 15$ V; $V_{GS} = 0$	$-C_{rs}$	<	0.75	0.75	pF
Transfer admittance (common source) $V_{DS} = 15$ V; $V_{GS} = 0$; f = 200 MHz	$\|y_{fs}\|$	>	3.2	3.2	$m\Omega^{-1}$
Noise figure at $V_{DS} = 15$ V; $V_{GS} = 0$ f = 100 MHz; $R_G = 1$ kΩ		<	2.5	2.5	dB
Equivalent noise voltage f = 10 Hz	$V_n/\sqrt{B}$	<	75	75	$nV/\sqrt{Hz}$

MECHANICAL DATA

Dimensions in mm

TO-72
Insulated electrodes

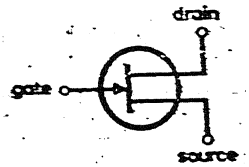

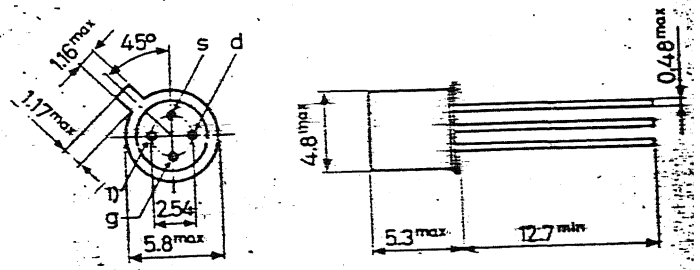

1) = shield lead (connected to case)

RATINGS Limiting values in accordance with the Absolute Maximum System (IEC 134)

Voltages				
Drain-source voltage	$\pm V_{DS}$	max.	30	V
Drain-gate voltage (open source)	V_{DGO}	max.	30	V
Gate-source voltage (open drain)	$-V_{GSO}$	max.	30	V
Currents				
Drain current	I_D	max.	20	mA
Gate current	I_G	max.	10	mA
Power dissipation				
Total power dissipation up to T_{amb} = 25 °C	P_{tot}	max.	300	mW
Temperatures				
Storage temperature	T_{stg}	−65 to +200		°C
Junction temperature	T_j	max.	200	°C

THERMAL RESISTANCE

From junction to ambient	$R_{th\ j\text{-}a}$	=	0.59	°C/

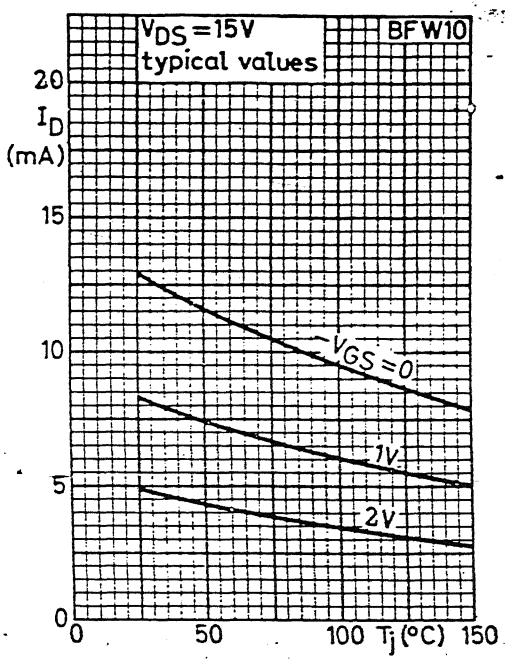
V_{DS} = 15V
typical values
BFW10
I_D (mA)
20
15
10
5
0
V_{GS} = 0
1V
2V
0
50
100
T_j (°C)
150

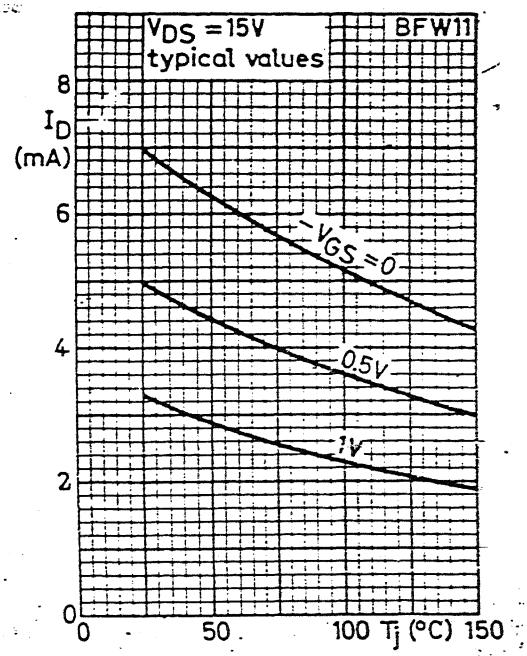
V_{DS} = 15V
typical values
BFW11
I_D (mA)
8
6
4
2
0
V_{GS} = 0
0.5V
1V
0
50
100
T_j (°C)
150

RCA Solid State Division

Linear Integrated Circuits

Monolithic Silicon

CA3127E

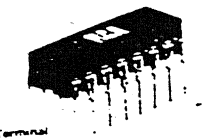

16-Lead Dual-In-Line Plastic Package H-1622

High-Frequency N-P-N Transistor Array

For Low-Power Applications at Frequencies up to 500 MHz

Features:

- Gain-Bandwidth Product (f_T) > 1 GHz
- Power Gain = 30 dB (typ.) at 100 MHz
- Noise Figure = 3.5 dB (typ.) at 100 MHz
- Five independent transistors on a common substrate

Applications:

- VHF amplifiers
- VHF mixers
- Multifunction combinations — RF/mixer/oscillator
- IF Converter
- IF amplifiers
- Sense amplifiers
- Synthesizers
- Synchronous detectors
- Cascade amplifiers

RCA-CA3127E* consists of five general-purpose silicon n-p-n transistors on a common monolithic substrate. Each of the completely isolated transistors exhibits low 1/f noise and a value of f_T in excess of 1 GHz, making the CA3127E useful from dc to 500 MHz. Access is provided to each of the terminals for the individual transistors and a separate substrate connection has been provided for maximum application flexibility. The monolithic construction of the CA3127E provides close electrical and thermal matching of the five transistors.

The CA3127E is supplied in a 16-lead dual-in-line plastic package and operates over the full military temperature range of −55 to +125°C.

*Formerly RCA Dev. No. TA6206.

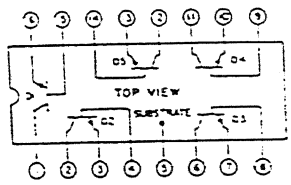

Fig. 1 – Schematic diagram of CA3127E.

MAXIMUM RATINGS, *Absolute-Maximum Values*, at T_A = 25°C

POWER DISSIPATION, P_D:

Any one transistor	85 mW
Total Package	
For T_A up to 75°C	425 mW
For T_A > 75°C Derate Linearly at	6.67 mW/°C

AMBIENT TEMPERATURE RANGE:

Operating	−55 to +125°C
Storage	−65 to +150°C

LEAD TEMPERATURE (DURING SOLDERING):

At distance 1/16 ± 1/32 inch (1.59 ± 0.79 mm) from case for 10 seconds max. +265°C

The following ratings apply for each transistor in the device.

Collector-to-Emitter Voltage, V_{CEO}	15 V
Collector-to-Base Voltage, V_{CBO}	20 V
Collector-to-Substrate Voltage, V_{CIO}*	20 V
Collector Current, I_C	20 mA

*The collector of each transistor of the CA3127E is isolated from the substrate by an integral diode. The substrate (terminal 5) must be connected to the most negative point in the external circuit to maintain isolation between transistors and to provide for normal transistor action.

CHARACTERISTICS CURVES
COMMON-EMITTER CONFIGURATION

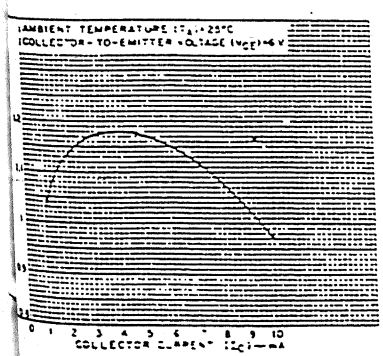

Fig. 4 – Gain-bandwidth product vs. collector current.

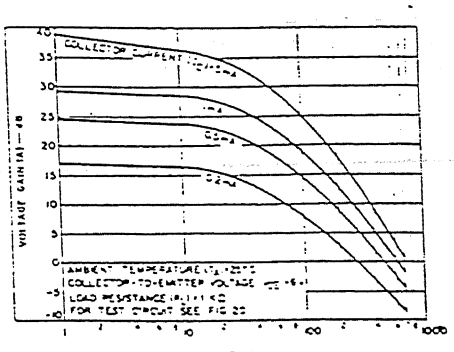

Fig. 6 – Voltage gain vs. frequency at R_L = 1 kΩ.

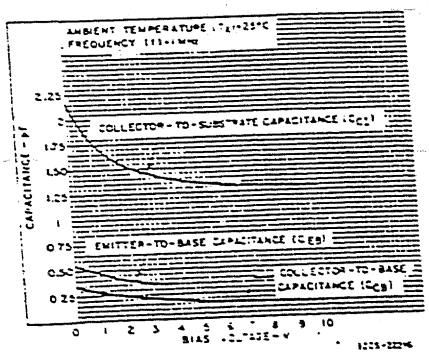

Fig. 5(a) – Capacitance vs. bias voltage for Q_2.

STATIC ELECTRICAL CHARACTERISTICS at $T_A = 25°C$

CHARACTERISTICS	SYMBOL	TEST CONDITIONS		LIMITS Min.	LIMITS Typ.	LIMITS Max.	UNITS
For Each Transistor:							
Collector-to-Base Breakdown Voltage	$V_{(BR)CBO}$	$I_C = 10\ \mu A, I_E = 0$		20	32	–	V
Collector-to-Emitter Breakdown Voltage	$V_{(BR)CEO}$	$I_C = 1\ mA, I_B = 0$		15	24	–	V
Collector-to-Substrate Breakdown Voltage	$V_{(BR)CIO}$	$I_{C1} = 10\ \mu A, I_B = 0, I_E = 0$		20	60	–	V
Emitter-to-Base Breakdown Voltage*	$V_{(BR)EBO}$	$I_E = 10\ \mu A, I_C = 0$		4	5.7	–	V
Collector-Cutoff-Current	I_{CEO}	$V_{CE} = 10\ V, I_B = 0$		–	–	0.5	µA
Collector-Cutoff-Current	I_{CBO}	$V_{CB} = 10\ V, I_E = 0$		–	–	40	nA
DC Forward-Current Transfer Ratio	h_{FE}	$V_{CE} = 6\ V$	$I_C = 5\ mA$	35	88	–	
			$I_C = 1\ mA$	40	90	–	
			$I_C = 0.1\ mA$	35	85	–	
Base-to-Emitter Voltage	V_{BE}	$V_{CE} = 6\ V$	$I_C = 5\ mA$	0.71	0.81	0.91	V
			$I_C = 1\ mA$	0.66	0.76	0.86	
			$I_C = 0.1\ mA$	0.60	0.70	0.80	
Collector-to-Emitter Saturation Voltage	$V_{CE(sat)}$	$I_C = 10\ mA, I_B = 1\ mA$		–	0.26	0.50	V
Magnitude of Difference in V_{BE}	$\lvert\Delta V_{BE}\rvert$	Q_1 & Q_2 Matched		–	0.5	5	mV
Magnitude of Difference in I_B	$\lvert\Delta I_B\rvert$	$V_{CE} = 6V, I_C = 1\ mA$		–	0.2	3	µA

*When used as a zener for reference voltage, the device must not be subjected to more than 0.1 millijoule of energy from any possible capacitive or electrostatic discharge in order to prevent degradation of the junction. Maximum operating zener current should be less than 10 mA.

DYNAMIC CHARACTERISTICS at $T_A = 25°C$

CHARACTERISTICS	SYMBOL	TEST CONDITIONS	Fig. No.	LIMITS Min.	LIMITS Typ.	LIMITS Max.	UNITS
I/F Noise Figure	NF	$f = 100\ kHz, R_S = 500\ \Omega$, $I_C = 1\ mA$	3	–	1.5	–	dB
Gain-Bandwidth Product	f_T	$V_{CE} = 6\ V, I_C = 5\ mA$	4	–	1.15	–	GHz
Collector-to-Base Capacitance	C_{CB}	$V_{CB} = 6\ V, f = 1\ MHz$	5	–	See Fig. 5	–	pF
Collector-to-Substrate Capacitance	C_{CI}	$V_{CI} = 6\ V, f = 1\ MHz$	5	–		–	pF
Emitter-to-Base Capacitance	C_{EB}	$V_{BE} = 4\ V, f = 1\ MHz$	5	–		–	pF
Voltage Gain	A	$V_{CE} = 6\ V, f = 10\ MHz$, $R_L = 1\ K\Omega, I_C = 1\ mA$	6, 18	–	25	–	dB
Power Gain	G_p	Cascode Configuration $f = 100\ MHz, V^+ = 12\ V$	19, 20	27	30	–	dB
Noise Figure	NF	$I_C = 1\ mA$	19, 20	–	3.5	–	dB
Input Resistance	h_{11}	Common-Emitter Configuration $V_{CE} = 6\ V$ $I_C = 1\ mA$ $f = 200\ MHz$	10	–	400	–	Ω
Output Resistance	h_{22}		10	–	4.6	–	kΩ
Input Capacitance	C_{11}		10	–	3.7	–	pF
Output Capacitance	C_{22}		10	–	2	–	pF
Magnitude of Forward Transadmittance	$\lvert Y_{21}\rvert$		14, 15	–	24	–	mmho

CHARACTERISTICS CURVES (Cont'd)
COMMON-EMITTER CONFIGURATION

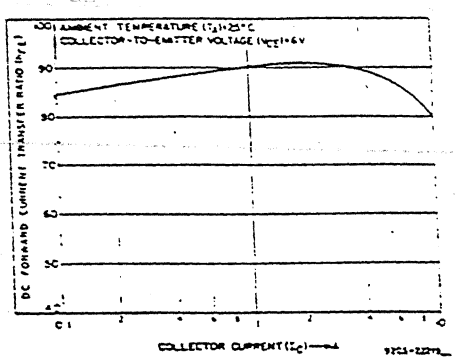

Fig. 6 — DC forward-current transfer ratio vs. collector current.

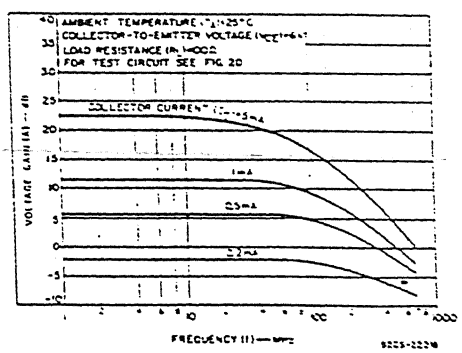

Fig. 7 — Voltage gain vs. frequency at $R_L = 100\ \Omega$.

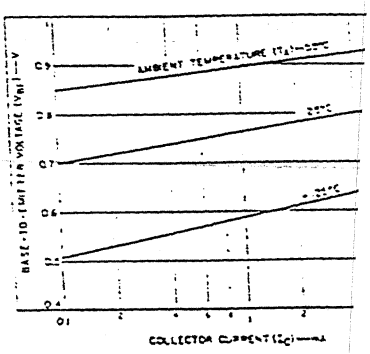

Fig. 9 — Base-to-emitter voltage vs. collector c

ICAL APPLICATIONS

FILTER NETWORKS

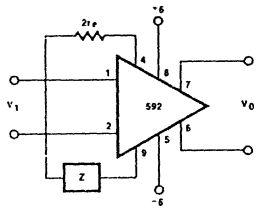

$$\frac{V_0(s)}{V_1(s)} \cong \frac{1.4 \times 10^4}{Z(s) + 2r_e}$$

$$\cong \frac{1.4 \times 10^4}{Z(s) + 32}$$

BASIC CONFIGURATION

Z NETWORK	FILTER TYPE	$V_0(s)$ TRANSFER $V_1(s)$ FUNCTION
R L	LOW PASS	$\frac{1.4 \times 10^4}{L}\left[\frac{1}{s + R/L}\right]$
R C	HIGH PASS	$\frac{1.4 \times 10^4}{R}\left[\frac{s}{s + 1/RC}\right]$
R L C	BAND PASS	$\frac{1.4 \times 10^4}{L}\left[\frac{s}{s^2 + R/L\, s + 1/LC}\right]$
L R C	BAND REJECT	$\frac{1.4 \times 10^4}{R}\left[\frac{s^2 + 1/LC}{s^2 + 1/LC + s/RC}\right]$

NOTE

In the networks above, the R value used is assumed to include $2r_e$, or approximately 32Ω.

DISC/TAPE PHASE MODULATED READBACK SYSTEMS

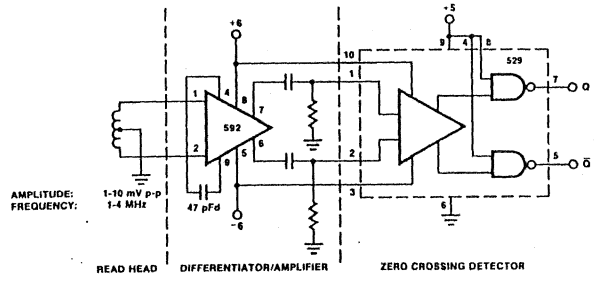

DIFFERENTIATION WITH HIGH COMMON MODE NOISE REJECTION

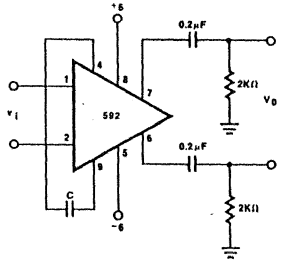

FOR FREQUENCY $F_1 \ll 1/2\pi(32)C$

$V_0 \cong 1.4 \times 10^4 C \frac{dV_i}{dT}$

DESCRIPTION

The 733 is a monolithic differential input, differential output, wideband video amplifier. It offers fixed gains of 10,100 or 400 without external components, and adjustable gains from 10 to 400 by the use of an external resistor. No external frequency compensation components are required for any gain option. Gain stability, wide bandwidth and low phase distortion are obtained through use of the classic series-shunt feedback from the emitter follower outputs to the inputs of the second stage. The emitter follower outputs provide low output impedance, and enable the device to drive capacitive loads. The 733 is intended for use as a high performance video and pulse amplifier in communications, magnetic memories, display and video recorder systems.

FEATURES

- **120MHz bandwidth**
- **250kΩ input resistance**
- **Selectable gains of 10,100 and 400**
- **No frequency compensation required**
- **Mil std 883A,B,C available**

PIN CONFIGURATION

F,N PACKAGE

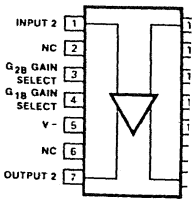

K PACKAGE

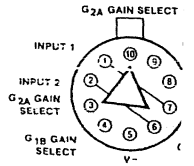

NOTE

Pin 5 connected to c

CIRCUIT SCHEMATIC

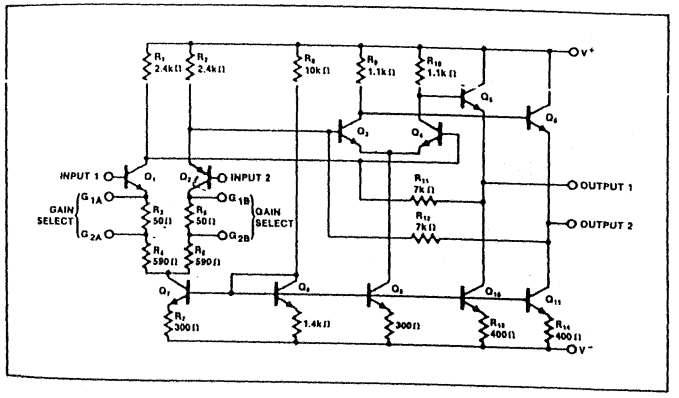

ABSOLUTE MAXIMUM RATINGS

PARAMETER	RATING	UNIT
Differential input Voltage	±5	V
Common mode input Voltage	±6	V
Vcc	±8	V
Output current	10	mA
Junction temperature	+150	°C
Storage temperature range	-65 to +150	°C
Operation temperature range		
μA733C	0 to +75	°C
μA733	-55 to +125	°C
Pd Power dissipation		
K package	300	mW
N F package	570	mW

T_A = +25°C, V_S = ±V, VCM = 0 unless otherwise specified.
Recommended operating supply voltages V_S = ±6.0V.

PARAMETER	TEST CONDITIONS	μA733C			μA733			UNITS
		Min	Typ	Max	Min	Typ	Max	
Differential voltage gain								
Gain 1[1]		250	400	600	300	400	500	V/V
Gain 2[2]	R_l = 2kΩ, V_{OUT} = 3Vp-p	80	100	120	90	100	110	V/V
Gain 3[3]		8.0	10	12	9.0	10	11	V/V
Bandwidth								
Gain 1[1]			40			40		MHz
Gain 2[2]			90			90		MHz
Gain 3[3]			120			120		MHz
Rise time								
Gain 1[1]			10.5			10.5		ns
Gain 2[2]	V_{OUT} = 1Vp-p		4.5	12		4.5	10	ns
Gain 3[3]			2.5			2.5		ns
Propagation delay								
Gain 1[1]			7.5			7.5		ns
Gain 2[2]	V_{OUT} = 1Vp-p		6.0	10		6.0	10	ns
Gain 3[3]			3.6			3.6		ns
Input resistance								
Gain 1[1]			4.0			4.0		kΩ
Gain 2[2]		10	30		20	30		kΩ
Gain 3[3]			250			250		kΩ
Input capacitance[2]	Gain 2		2.0			2.0		pF
Input offset current			0.4	5.0		0.4	3.0	μA
Input bias current			9.0	30		9.0	20	μA
Input noise voltage	BW = 1kHz to 10MHz		12			12		μVrms
Input voltage range		±1.0			±1.0			V
Common mode Rejection ratio								
Gain 2	VCM = ±V, f ≤ 100kHz	60	86		60	86		dB
Gain 2	VCM = ±1V, F = 5MHz		60			60		dB
Supply voltage Rejection ratio								
Gain 2	ΔVs = ±0.5V	50	70		50	70		dB
Output offset voltage								
Gain 1[1]	R_L = ∞		0.6	1.5		0.6	1.5	V
Gain 2 and 3[2,3]			0.35	1.5		0.35	1.0	V
Output common mode voltage	R_L = ∞	2.4	2.9	3.4	2.4	2.9	3.4	V
Output voltage swing	R_L = 2k	3.0	4.0		3.0	4.0		
Output sink current		2.5	3.6		2.5	3.6		mA
Output resistance			20			20		Ω
Power supply current	R_L ± ∞		18	24		18	24	mA

NOTES
1. Gain select pins G_{1A} and G_{1B} connected together
2. Gain select pins G_{2A} and G_{2B} connected together
3. All gain select pins open

Rmi
4,11
3,12
NA.

TYPICAL PERFORMANCE CHARACTERISTICS

PHASE SHIFT AS A FUNCTION OF FREQUENCY

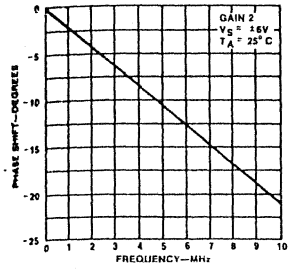

PHASE SHIFT AS A FUNCTION OF FREQUENCY

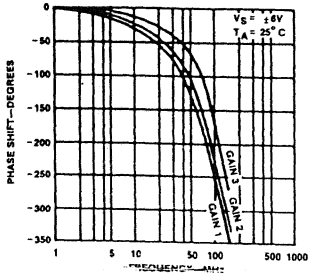

VOLTAGE GAIN AS FUNCTION OF FREQUE

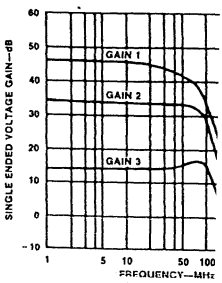

COMMON MODE REJECTION RATIO AS A FUNCTION OF FREQUENCY

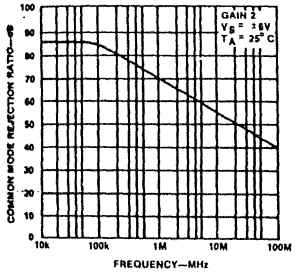

OUTPUT VOLTAGE SWING AS A FUNCTION OF FREQUENCY

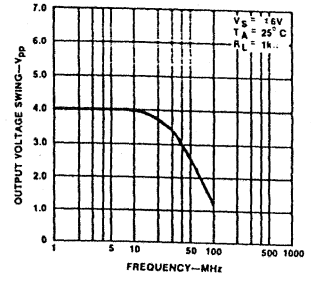

PULSE RESPONS

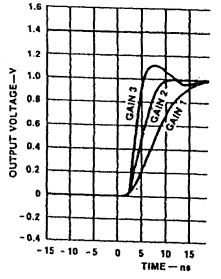

DIFFERENTIAL OVERDRIVE RECOVERY TIME

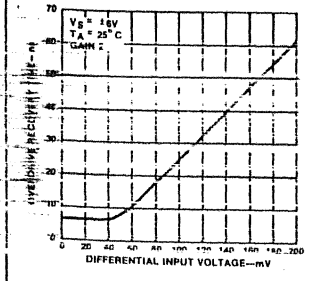

PULSE RESPONSE AS A FUNCTION OF SUPPLY VOLTAGE

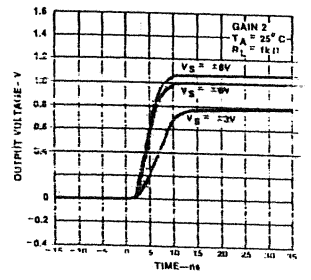

PULSE RESPONS AS A FUNCTIOI OF TEMPERATUI

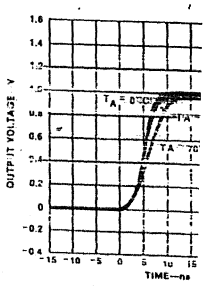

CAL PERFORMANCE CHARACTERISTICS (Cont'd)

VOLTAGE GAIN AS A FUNCTION OF TEMPERATURE

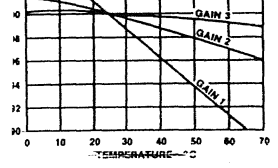

GAIN vs FREQUENCY AS A FUNCTION OF TEMPERATURE

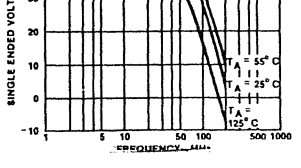

VOLTAGE GAIN AS A FUNCTION OF SUPPLY VOLTAGE

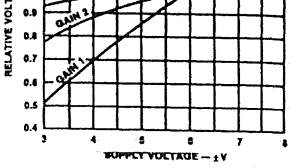

GAIN vs FREQUENCY AS A FUNCTION OF SUPPLY VOLTAGE

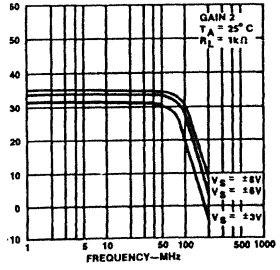

VOLTAGE GAIN ADJUST CIRCUIT

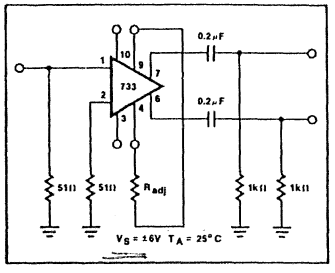

(Pin numbers apply to K Package)

VOLTAGE GAIN AS A FUNCTION OF RADJ (FIGURE 3)

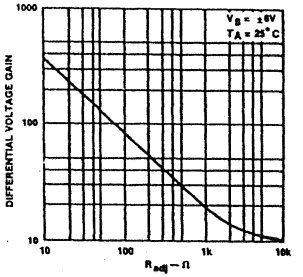

SUPPLY CURRENT AS A FUNCTION OF TEMPERATURE

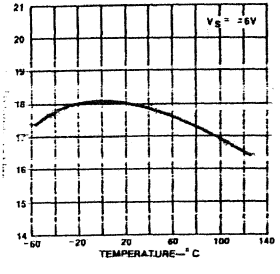

SUPPLY CURRENT AS A FUNCTION OF SUPPLY VOLTAGE

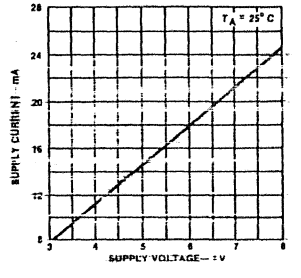

OUTPUT VOLTAGE AND CURRENT SWING AS A FUNCTION OF SUPPLY VOLTAGE

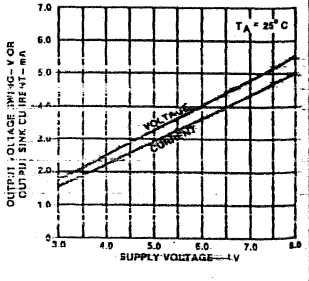

TYPICAL PERFORMANCE CHARACTERISTICS (Cont'd)

OUTPUT VOLTAGE SWING AS A FUNCTION OF LOAD RESISTANCE

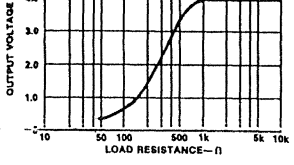

INPUT RESISTANCE AS A FUNCTION OF TEMPERATURE

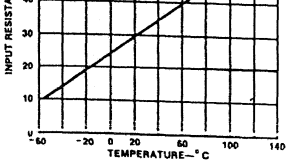

INPUT NOISE VOLT AS A FUNCTION OF SOURCE RESIST

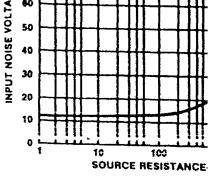

TEST CIRCUITS T_A = 25°C unless otherwise specified.

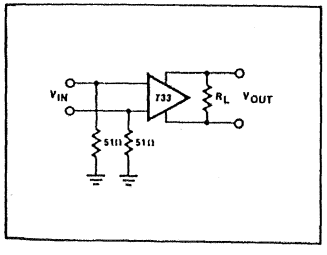

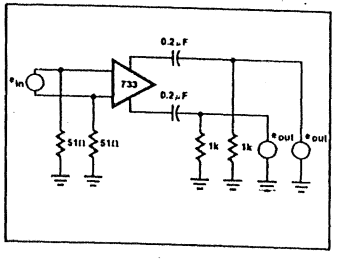

ATIONS

e main features of the device is that oltages (V1+, V1−) need not be as indicated in the following dia- r proper operation, however, neg- ly (V1−) should always be at least more negative than the ground pin 6). Input Common Mode range e limited to values of two volts less supply voltages (V1+ and V1−) up to um of ±6 volts as supply voltages ased.

mportant to note that Output A is in th Input A and Output B is in phase ut B.

AL APPLICATIONS

PHOTODIODE DETECTOR

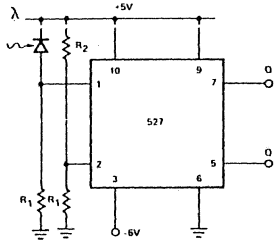

ECL TO TTL INTERFACE

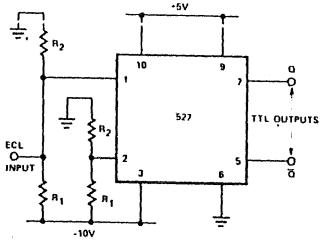

MOS MEMORY SENSE AMP

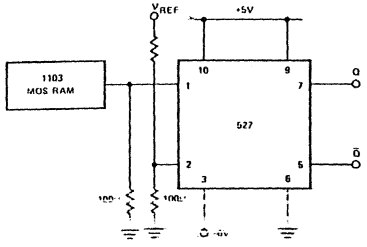

TTL TO ECL INTERFACE

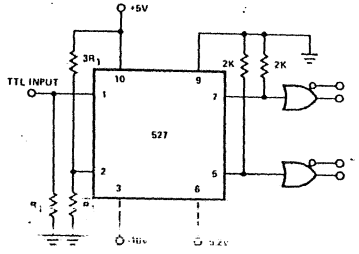

DESCRIPTION

The SE/NE529 is a high speed analog voltage comparator which, for the first time unites state-of-the-art Schottky diode technology with the conventional linear process. This allows simultaneous fabrication of high speed T²L gates with a precision linear amplifier on a single monolithic chip.

FEATURES

- **10ns propagation delay**
- **Complementary output gates**
- **TTL or ECL compatible outputs**
- **Wide common mode and differential voltage range**

APPLICATIONS

- **A/D conversion**
- **ECL to TTL interface**
- **TTL to ECL interface**
- **Memory sensing**
- **Optical data coupling**
- **Mil std 883A,B,C available**

PIN CONFIGURATION

F,N PACKAGE

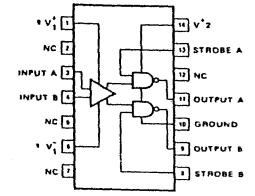

K PACKAGE

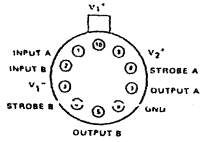

ABSOLUTE MAXIMUM RATINGS

PARAMETER	RATING	UNIT
Positive supply voltage (V1+)	+15	V
Negative supply voltage (V1−)	−15	V
Gate supply voltage (V2+)	+7	V
Output voltage	+15	V
Differential input voltage	±5	V
Input common mode voltage	±6	V
Power dissipation	600	mW
Operating temperature range		
NE529	0 to +70	°C
SE529	−55 to +125	°C
Storage temperature range	−65 to +150	°C
Lead temperature (soldering, 60 sec)	+300	°C

BLOCK DIAGRAM

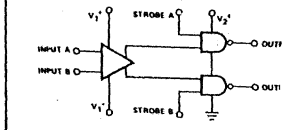

EQUIVALENT SCHEMATIC

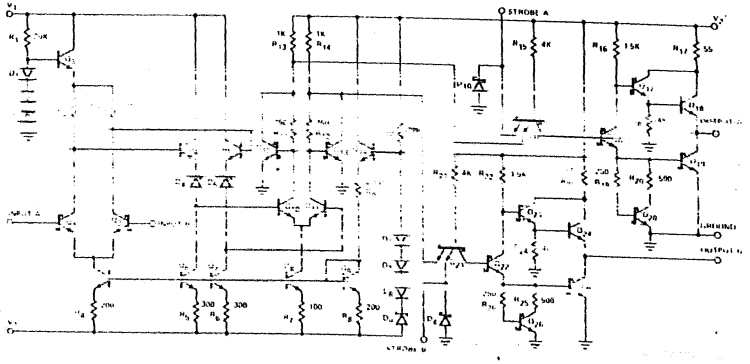

CTRICAL CHARACTERISTICS $V_1+ = +10V, V_2+ = +5.0V, V_1- = -10V, V_{IN} = 0V$ unless otherwise specified.

PARAMETER	TEST CONDITIONS	SE529			NE529			UNIT
		Min	Typ	Max	Min	Typ	Max	
CHARACTERISTICS								
offset voltage @25°C				4			6	mV
r temperature range				6			10	mV
bias current @25°C	$V_1+ = 10V, V_1- = -10V$		5	12		5	20	µA
r temperature range	$V_{IN} = 0V$			36			50	µA
offset current @25°C	$V_1+ = 10V, V_1- = -10V$		2	3		2	5	µA
r temperature range	$V_{IN} = 0V$			9			15	µA
impedance	$T_A = 25°C$, f = 1kHz		10			10		kΩ
CHARACTERISTICS								
ut voltage								
state	$V_2+ = 4.75V, I_{source} = -1mA$	2.5	3.3		2.7	3.3		V
state	$V_2+ = 4.75V, I_{sink} = 10mA$			0.5			0.5	V
e inputs								
input current	$V_2+ = 5.25V, V_{strobe} = 0.5V$			-2			-2	mA
input current @25°C	$V_2+ = 5.25V, V_{strobe} = 2.7V$			50			100	µA
er temperature range	$V_2+ = 5.25V, V_{strobe} = 2.7V$			200			200	µA
input voltage	$V_2+ = 4.75V$			0.8			0.8	V
input voltage	$V_2+ = 4.75V$	2.0			2.0			V
t circuit								
utput current	$V_2+ = 5.25V, V_{OUT} = 0V$	-18		-70	-18		-70	mA
ER SUPPLY REQUIREMENTS								
ply voltage								
+		5		10	5		10	V
-		-6		-10	-6		-10	V
+		4.5	5	5.5	4.75	5	5.25	V
ply current	$V_1+ = 10V, V_1- = -10V$ $V_2+ = 5.25V$							
+	Over temp.			5			5	mA
-	Over temp.			10			10	mA
+	Over temp.			20			20	mA

ECTRICAL CHARACTERISTICS $T_A = 25°C$

PARAMETER	TEST CONDITIONS	LIMITS			UNIT
		Min	Typ	Max	
sient response	$V_{IN} = \pm 100mV$ step				
agation delay time					
LH			12	22	ns
HL			10	20	ns
y between output			2	5	ns
and E					
be delay time					
N turn-on time			6		ns
FF turn-off time			6		ns

ers are guaranteed over the temperature range unless otherwise specified.

TYPICAL PERFORMANCE CHARACTERISTICS

INPUT CURRENTS vs TEMPERATURE

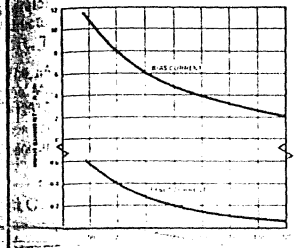

SUPPLY CURRENT vs TEMPERATURE

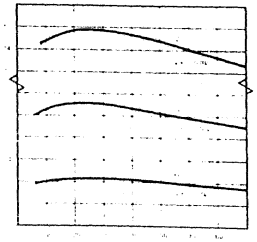

POWER DISSIPATION vs SUPPLY VOLTAGE

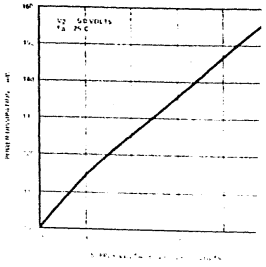

SUPPLY CURRENT vs SUPPLY VOLTAGE

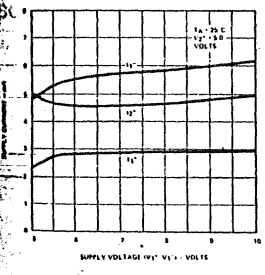

OUTPUT PROPAGATION DELAYS

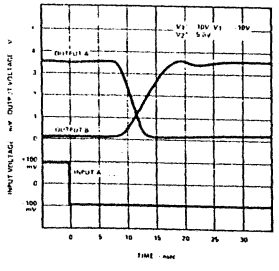

RESPONSE TIME FOR VARIOUS INPUT OVERDRIVE

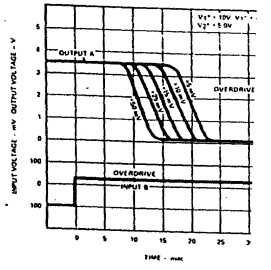

Micro-Cap Evaluation 6.1.9
Saju Thomas, IITK
AC Analysis of PREAMPLIFIER

Frequency Range 1E8,1000
Number of Points 51
Temperature Linear 27
Maximum Change % 5
Noise Input NONE
Noise Output 2
Run Options Save
State Variables Zero
Frequency Step Log
Operating Point On

Temperature = 27 Case= 1

DC Operating Point Values

DC Operating Point Voltages

Node	Voltage	Node	Voltage	Node	Voltage
1	4.70	2	4.71u	3	6.30m
4	10.46	5	12.00	6	12.00
7	4.71u	8	7.85	9	5.96
10	6.04	11	5.15	12	11.24
13	6.04	14	5.23	15	5.15
16	11.25	17	0.00		

Bipolar Junction Transistors

	Q1	Q2
Model	CA3127	CA3127
IB	35.40u	32.61u
IC	3.40m	3.40m
VBE	812.72m	810.55m
VBC	-77.83m	-1.81
VCE	890.55m	2.63
BETADC	96.03	104.37
GM	131.28m	131.43m
RPI	730.59	793.18
RX	15.00	15.00
RO	5.88K	6.39K
CPI	18.65p	18.67p
CMU	398.77f	269.08f
CBX	0.00	0.00
CJS	1.05p	975.05f
BETAAC	95.91	104.24
FT	1.10G	1.10G
Power Terms:		
PD	3.06m	8.96m
PS	0.00	0.00
Pin Currents:		
Ib	35.40u	32.61u
Ic	3.40m	3.40m
Ie	-3.44m	-3.44m
Is	0.00	0.00
Condition:		
State	LIN	LIN

JFET Devices

	J1
Model	BFW10
ID	10.28m
VGS	4.71u
VDS	4.70
GM	5.83m
GDS	66.79u
CGS	4.50p
CGD	4.19p

Power Terms:

PD	48.32m
PS	0.00

Pin Currents:

Ig	-4.71p
Id	10.28m
Is	-10.28m

Condition:

State	SAT

Resistor Devices

	R1	R2	R3	R4	R6
Power Terms:					
PD	0.02f	39.69p	59.21m	15.86m	186.54f
Pin Currents:					
Ir	-4.71p	-6.30n	-10.28m	-10.28m	-6.30n

	R7	R8	R9	R10	R11
Power Terms:					
PD	1.00E-105	17.68m	18.01m	2.64m	106.18n
Pin Currents:					
Ir	0.00	-3.43m	-3.47m	-3.47m	32.59u

	R12	R13	R14	R15	R16
Power Terms:					
PD	2.75u	17.68m	259.36u	11.57m	2.54m
Pin Currents:					
Ir	-35.38u	3.43m	3.43m	3.40m	3.40m

	R17
Power Terms:	
PD	1.00E-103
Pin Currents:	
Ir	0.00

Capacitor Devices

	C1	C2	C3	C4	C5
Power Terms:					
PS	0.00	0.00	0.00	0.00	0.00
Pin Currents:					
Ic	0.00	0.00	0.00	0.00	0.00

	C6	C7	C8	C9	C10
Power Terms:					
PS	0.00	0.00	0.00	0.00	0.00
Pin Currents:					
Ic	0.00	0.00	0.00	0.00	0.00